Activation of Water Molecule. 2. Generation of Strong Hydroxo Bases by the Reaction of Water with Platinum(0) Phosphine Complexes and the Applications as Catalysts for H–D Exchange and Hydration Reactions

Toshikatsu Yoshida, Tadao Matsuda, Tamon Okano, Tetsumi Kitani, and Sei Otsuka*

Contribution from the Department of Chemistry, Faculty of Engineering Science, Osaka University, Toyonaka, Osaka, Japan 560. *Received April 3, 1978*

Abstract: The dissociation of $Pt(PEt_3)_4$ in organic solvents (THF, *n*-heptane) occurs to give $Pt(PEt_3)_3$ (K_L = 0.5 M in THF at 20 °C), no further dissociation being detected, while $Pt[P(i\text{-}Pr)_3]_3$, upon dissolution in the above solvents, exists mainly as $Pt[P(i\text{-}Pr)_3]_2$ (K_L = 0.14 M in THF at 20 °C). Addition of water to PtL_3 (L = PEt_3, $P(i\text{-}Pr)_3$) generates strong hydroxy bases, $[PtHL_3]OH$ (L = PEt_3) or *trans*-$[PtH(S)L_2]OH$ (L = $P(i\text{-}Pr)_3$, S = solvent), while the addition to $Pt[P(i\text{-}Pr)_3]_2$ gives a σ-hydrido hydroxo compound, *trans*-$PtH(OH)[P(i\text{-}Pr)_3]_2$. Quantitative study on the reversible water addition to PtL_3 in organic solvents was carried out by pH and conductance measurements. The conductometric behaviors of the system PtL_3 (L = PEt_3)/H_2O in pyridine and THF are described in terms of two equilibria: (1) $PtL_3 + H_2O \rightleftharpoons [PtHL_3]OH$, K_0; (2) $[PtHL_3]OH \rightleftharpoons [PtHL_3]^+ + OH^-$, K_d (K_0 = 0.6 (0.3) M^{-1}, $K_d = 4.2\ (0.2) \times 10^{-2} \exp(-11.9(0.1)/[H_2O])$ M in pyridine at 0.5 °C). The system PtL_3 (L = $P(i\text{-}Pr)_3$)/H_2O involved (1) $PtL_3 \rightleftharpoons PtL_2 + L$, K_L, vide supra; (2) $PtL_2 + H_2O \rightleftharpoons PtH(OH)L_2$, K_0; (3) $PtH(OH)L_2 + S \rightleftharpoons [PtH(S)L_2]OH$, K_s; (4) $[PtH(S)L_2]OH \rightleftharpoons [PtH(S)L_2]^+ + OH^-$, K_d (only composite constants can be calculated, $(1 + K_s)K_0$ = 0.1 (0.06) M^{-1}, $K_sK_d/(1 + K_s) = 1.2\ (0.1) \times 10^{-1} \exp(-20.8(0.2)/[H_2O])$ M in pyridine at 0.5 °C). Systems with PtL_3/H_2O proved to be efficient catalysts for H–D exchange of organic substances and for hydration of organic unsaturated bonds. Thus, activated C–H bonds such as α-hydrogen atoms of ketones, aldehydes, sulfones, sulfoxides, and nitroalkanes undergo the H–D exchange. The mechanism was studied for H–D exchange of $C_6H_5COCH_3$ to show that the reaction follows a rate equation, $R = k[Pt][C_6H_5COCH_3]$, and involves a reversible condensation, $M^+OD^- + C_6H_5COCH_3 \rightleftharpoons MCH_2COC_6H_5 + DHO$, as the rate-determining step. Unlike the alkaline base-catalyzed reaction, α-olefinic, allylic, and aldehydic hydrogen atoms of α,β-unsaturated carbonyl compounds were exchanged. The hydration of the nitrile and double bonds of RCH=CHCN catalyzed by $[PtHL_3]OH$ or $[PtH(S)L_2]OH$ and *trans*-$Pt(OH)(R)(PPh_3)_2$ occurs with excellent chemical yields.

Oxidative addition of protic compounds to low-valent transition metal complexes is known to give a variety of metal hydrido complexes.[1] The fates of unstable HMOR species initially formed by an alcohol addition have been studied to discern β-hydrogen elimination[2-4] and sometimes a decarbonylation reaction.[5,6] Water should give HMOH species. In fact, the reactions with $Os_3(CO)_{12}$ and $[Rh(en)_2]^+$ were reported to give $Os_3(H)(OH)(CO)_{10}$[7] and $[RhH(OH)(en)_2]^+$,[8] respectively. The reaction of $Pt(PEt_3)_3$ with water yields an unstable species $[PtH(PEt_3)_3]OH$,[9] which was not isolated. The instability suggests an unfavorable formation constant. However, no quantitative information is available for the addition–elimination equilibrium.

$$M + H_2O \rightleftharpoons HMOH$$

The chemistry of hydrido hydroxo metal compounds in general remains practically unexplored. The species may be obtained through alternative routes other than the water addition. For example, $RuH(OH)(S)(PPh_3)_2$ (S = H_2O, THF) was prepared by treating $RuHCl(PPh_3)_3$ with OH^-.[10] Our present concern is the oxidative addition reaction of water. One incentive arises from the current problem of water-mediated energy conversion and another from the possible application of the MHOH species for organic synthesis.

Some square planar hydroxo compounds $M(OH)(R)L_2$ (M = Pd, Pt; R = haloalkenyl, aryl, etc; L = PR_3) undergo a facile condensation reaction with active methyl- or methylene-containing compounds,[3,11-13] leading to the corresponding σ-alkyl metal complexes, a fact indicative of considerable nucleophilicity of the OH moiety. We have shown[12] that the enhanced nucleophilicity is strongly associated with the trans influence of R. The hydride being known as a strong trans-influencing ligand,[14] we expect *trans*-$PtH(OH)L_2$ (L = *tert*-alkylphosphine) to be a strong nucleophile; such a species should readily be generated by adding water to relevant metal compounds, e.g., ML_n (M = Pd, Pt; n = 2, 3).[15,16] In fact, we could isolate *trans*-$PtH(OH)[P(i\text{-}Pr)_3]_2$ from the system $Pt[P(i\text{-}Pr)_3]_2/H_2O$. The systems PtL_n/H_2O were found to be powerful bases as expected. The basic site of the ML_n/H_2O systems, however, needs to be clarified, since ML_n (M = Pd, Pt; n = 2, 3) itself exhibits strong σ and π basicities due to the filled nonbonding orbitals. A pertinent question here remains: what is the species responsible for the basicity, H^-, OH^-, or the metal center? Perhaps the basic site varies depending on the nature of the acid (acceptor). Hence in this paper we shall first examine quantitatively the solution behavior of ML_n in aprotic organic solvents containing water by conductometric means. The solution chemistry of closely related *trans*-$Pt(OH)(Ph)(PPh_3)_2$ is also investigated.

The strong basicity in aprotic media promises extensive utility. Of many possible applications it was shown that the $Pt[P(i\text{-}Pr)_3]_3/H_2O$ system serves as a catalyst for the water gas shift reactions, effective at substantially lower temperature[17] than conventional heterogeneous catalysis. We wish to report here utilization of the systems ML_n/H_2O as catalysts for H–D exchange of active C–H compounds with D_2O and for hydration of nitriles to amides. Emphasis will be given to the differences in chemical behavior between these systems and the conventional alkaline hydroxide.

Experimental Section

^1H NMR, IR, mass, and electronic spectra were recorded with a JEOL JNM-4H-100, a Hitachi Model 295 spectrometer, a Hitachi RMS-4 mass spectrometer, and a Hitachi EPS-3T spectrophotometer, respectively. Quartz cells employed have a ground-joint stopper carrying a three-way cock to prevent air. The pH measurements were made on a Hitachi-Horiba pH meter, Model H-5. The vessels employed were of the Schlenk type. All reactions and physical measurements were carried out under a pure nitrogen or argon atmosphere. Extreme care to prevent air in any phase is necessary to obtain reliable optical and conductometric data, since all the Pt(0) complexes employed in the present study are highly air sensitive. The following

0002-7863/79/1501-2027$01.00/0

Table I. Conductances of PtL_3 in Pyridine-H_2O Mixture[a]

H_2O concn, M	$Pt(PEt_3)_3$ concn, 10^{-4} M	Λ[b]	H_2O concn, M	$Pt[P(i\text{-}Pr)_3]_3$ concn, 10^{-4} M	Λ[b]
5.549	2.05	17.3	5.549	1.18	14.4
5.549	2.45	17.3	5.549	2.00	13.8
5.549	3.26	16.2	5.549	2.67	13.7
5.549	4.08	16.8	5.549	3.92	12.7
5.549	6.12	15.7	5.549	5.88	11.5
5.549	8.16	15.4			
0.550	8.16	3.52	1.110	7.84	1.71
1.110	8.16	4.52	2.775	7.84	4.47
1.665	8.16	6.31	3.330	7.84	5.46
1.942	8.16	6.84	3.885	7.84	7.07
2.220	8.16	9.07	4.162	7.84	7.10
2.497	8.16	10.2	4.440	7.84	10.1
2.775	8.16	13.0	4.994	7.84	10.8
3.052	8.16	14.0	5.549	7.84	11.7
3.330	8.16	14.3	6.104	7.84	11.7
3.885	8.16	16.0	7.214	7.84	11.3
5.549	8.16	15.4	7.769	7.84	10.5
			8.324	7.84	10.5

[a] Measured at 0.5 °C. [b] Λ is observed equivalent conductance in Ω^{-1} cm^2.

complexes were prepared by known methods: $M(PEt_3)_4$ (M = Ni,[16] Pd,[16] Pt[16]), PtL_3 (L = PEt_3,[18] $P(i\text{-}Pr)_3$,[15] PPh_3[19]), ML_2 (M = Pd, L = $P(c\text{-}C_6H_{11})_3$;[15] M = Pt, L = $P(i\text{-}Pr)_3$,[15] $P(c\text{-}C_6H_{11})_3$,[15] $PPh(t\text{-}Bu)_2$[15]), *trans*-Pt(OH)(R)$(PPh_3)_2$[12] (R = CCl=CCl_2, CH=CCl_2, Ph), and *trans*-Pt(CH_2COPh)(Ph)$(PPh_3)_2$.[12] (*S*)-(+)-Methyldeoxybenzoin, $[\alpha]^{21}{}_D$ 54.0° (*c* 3.54, $CHCl_3$), was prepared according to the conventional method;[20] the optical purity was 27%. All liquid organic compounds were distilled under a pure nitrogen atmosphere before use.

Determination of Ligand Dissociation Constants of PtL_4 (L = PEt_3) and PtL_3 (L = $P(i\text{-}Pr)_3$). Ligand dissociation constants were determined spectroscopically using jacketed cells to secure constant temperature (±0.5 °C). Electronic spectra were recorded in the range 340–520 nm in *n*-heptane and THF at 20 °C. Beer's law was checked over a 100-fold variation in complex concentration. Almost complete dissociation of 1 mol of the ligand from $Pt(PEt_3)_4$ or $Pt[P(i\text{-}Pr)_3]_3$ occurs upon high dilution. The stoichiometry of ligand dissociation was confirmed by observation of two isosbestic points for the solutions of $Pt(PEt_3)_4$ and $Pt[P(i\text{-}Pr)_3]_3$ with and without added phosphines (see text). Dissociation constants were determined assuming complete dissociation at high dilution (2.5×10^{-3} to 4.9×10^{-3} M) and the absence of ligand dissociation in the presence of a large excess of added phosphine ([ligand]/[complex] = 380–670).

Conductance Measurements. A Yanagimoto Conductivity Outfit Model MY-7 (range 0.1–10^{-6} Ω) and a conductivity cell with sealed-in platinum electrodes were used for conductance measurements. The cell constant determined with a 0.01 M aqueous KCl solution in the conventional manner[21] was 0.529 cm^{-1}. The purity of dry solvents used (pyridine, THF, and acetone) was carefully monitored via resistance measurements. Their specific conductances were less than 5×10^{-7} Ω^{-1} cm^{-1}. The corresponding values of aqueous pyridine, THF, and acetone with varying water concentration (1–25 M) were also less than 4×10^{-7} Ω^{-1} cm^{-1}. Conductivity measurements were carried out at 0.5 °C for aqueous pyridine solutions of PtL_3 (L = PEt_3, $P(i\text{-}Pr)_3$) and their conductances at various complex and H_2O concentrations are shown in Table I.

Preparation of {PtH(pyridine)[P(*i*-Pr)$_3$]$_2$}BF$_4$. A solution of $NaBF_4$ (0.15 g, 1.37 mmol) in H_2O (2 mL) was added to a mixture of $Pt[P(i\text{-}Pr)_3]_3$ (0.46 g, 0.68 mmol), H_2O (3 mL), and pyridine (10 mL) at room temperature. The resulting colorless solution was evaporated in vacuo and the solid residue was extracted with benzene. Concentration of the extract gave colorless crystals (0.16 g, 35%): mp 134–135 °C; IR (Nujol) 2230 cm^{-1} ν(Pt–H); ^{1}H NMR ($CDCl_3$) δ −18.9 (t, Pt–H, $J_{P\text{-}H}$ = 14.2, $J_{Pt\text{-}H}$ = 1006 Hz), 1.20 (q, CH_3, $^3J_{H\text{-}P} + {}^5J_{H\text{-}P}$ = 14.7, $J_{H\text{-}H}$ = 7.3 Hz), 2.12 (m, CH), 7–8.25 and 8.70 (m, pyridine).

Anal. ($C_{23}H_{48}BF_4NP_2Pt$) C, H, N.

Preparation of *trans*-PtH(OH)[P(*i*-Pr)$_3$]$_2$. To a solution of $Pt[P(i\text{-}Pr)_3]_2$ (0.31 g, 0.6 mmol) in THF (10 mL) was added H_2O (4 mL) at room temperature. After stirring for 0.5 h, the pale yellow solution was concentrated in vacuo to give colorless crystals together with untractable brown oil. The concentrated residue was extracted with *n*-pentane (10 mL) at 0 °C and the brown extract was concentrated to 3 mL in vacuo under cooling (−10 °C). On standing at −35 °C, colorless crystals were separated (0.06 g, 18%). The compound can be stored in a freezer for several weeks, but decomposes above room temperature.

Anal. ($C_{18}H_{44}OP_2Pt$) C, H.

Attempts to isolate *trans*-PtH(OH)[P(*i*-Pr)$_3$]$_2$ from a pale yellow mixture of $Pt[P(i\text{-}Pr)_3]_3$ (0.27 g, 0.52 mmol) and H_2O (2 mL) in THF (5 mL) by a similar procedure as above failed; $Pt[P(i\text{-}Pr)_3]_3$ was recovered almost quantitatively.

Hydrolysis of *trans*-Pt(CH$_2$COPh)(Ph)(PPh$_3$)$_2$. A mixture of *trans*-Pt(CH_2COPh)(Ph)$(PPh_3)_2$ (0.046 g, 0.05 mmol) and H_2O (1 mL) in THF (5 mL) was heated at 70 °C for 2 h. After concentration in vacuo, the residue was recrystallized from a mixture of toluene and *n*-hexane to give *trans*-Pt(OH)(Ph)$(PPh_3)_2$ (0.03 g, 71%) as colorless crystals.

H–D Exchange Reactions. Some typical examples are given below.

I. PhCOCH$_3$. A mixture of $Pt(PEt_3)_3$ (50 mg, 0.09 mmol), $PhCOCH_3$ (1.0 g, 8.3 mmol), and D_2O (0.78 mL, 43 mmol) in THF (3 mL) was heated at 80 °C for 20 h. After deactivation of the catalyst by exposing to air, the reaction mixture was concentrated under reduced pressure (15 mmHg) at ambient temperature. The deuterated acetophenone was isolated by distillation of the concentrated residue in 80–90% yield. The absolute intensity of ^{1}H NMR signals was determined by employing an $AlMe_3$ solution (0.129 M in toluene-d_8) as external reference. The ^{1}H NMR (1.31 M in CCl_4) showed CH_3 (δ 2.55, m) and Ph proton signals (δ 7.48, m) in a relative intensity of 0.6:5.0. The percent deuteration of the methyl and phenyl group was calculated to be 80 and 0, respectively. The mass spectrum indicated the corrected relative intensity of four parent isotope ions to be 0.5 (M), 13.9 (M + 1), 48.6 (M + 2), and 56.4 (M + 3). The deuterium distribution calculated from this relative intensity was d_0, 1.3; d_1, 11.5; d_2, 40.4; d_3, 46.8%. The total deuterium incorporated into $PhCOCH_3$, i.e., percent deuteration, calculated from these values was 78%, which is in good agreement with the value obtained from ^{1}H NMR. The observed relative intensity of two isotope ions of $PhCO^+$ (M′) were 1 (M′) and 0.087 (M′ + 1), which is identical with that of undeuterated acetophenone. These also indicate no deuterium incorporation into the phenyl group.

II. PhCOCH$_2$CH$_3$. A similar exchange reaction catalyzed by $Pt(PEt_3)_3$ gave 83% deuteration with 80% isolated yield after heating at 80 °C for 20 h. The deuterium incorporation in phenyl and β-methyl group was absent. The corrected relative intensities of three parent isotope ions were 3.7 (M), 20.1 (M + 1), and 41.2 (M + 2).

III. Benzalacetone. Benzalacetone was deuterated by catalysis with $Pt(PEt_3)_3$ under similar conditions as mentioned above to give deuterated benzalacetone quantitatively. The relative intensity of α-CH_3 (δ 2.35, m), α-CH= (δ 6.70, m), and the sum of β-CH= and Ph proton signals (δ 7.40, m, 7.48, m) were 1.32, 0.36, and 6.00, suggesting percent exchange of α-CH_3 and α-CH= protons to be 56 and 64, respectively. The corrected relative intensities of five parent isotope ions were 24.3 (M), 71.2 (M + 1), 117.9 (M + 2), 108.4 (M + 3), and 50.4 (M + 4). The *d* distribution was d_0, 6.8; d_1, 19.1; d_2, 31.4; d_3, 28.9; d_4, 13.8%. The percent exchange was 56, which was in good agreement with the corresponding value (58%) evaluated on the basis of the ^{1}H NMR data. Under the same condition but employing aqueous NaOH as catalyst, only methyl-deuterated benzalacetone was obtained. The *d* distribution was d_0, 61.8; d_1, 29.1; d_3, 7.0; d_3, 2.1; d_4, 0%. The ^{1}H NMR gives percent exchange of α-CH_3 and α-olefinic protons to be 22 and 0%, respectively.

IV. Phenyl Propenyl Ketone. Similarly phenyl propenyl ketone was deuterated by catalysis with $Pt(PEt_3)_3$ under similar conditions as above to give deuterated phenyl propenyl ketone quantitatively. The relative intensities of Ph (δ 7.48, m), the sum of α- and β-CH= (δ 6.85, m), and γ-CH_3 proton signals (δ 1.82, m) were 5.00:1.18:1.97.

V. Cinnamaldehyde. Deuterated cinnamaldehyde was obtained under similar conditions employing $Pt(PEt_3)_3$ as catalyst in 60% yield. The relative intensities of aldehydic (δ 9.58, m), α-CH= (δ 6.54, m), and sum of phenyl and β-CH= proton signals (δ 7.33, m) were 0.84:0.65:6.00, suggesting the percent exchange of aldehydic and α-CH= protons to be 14 and 35, respectively. The corrected relative

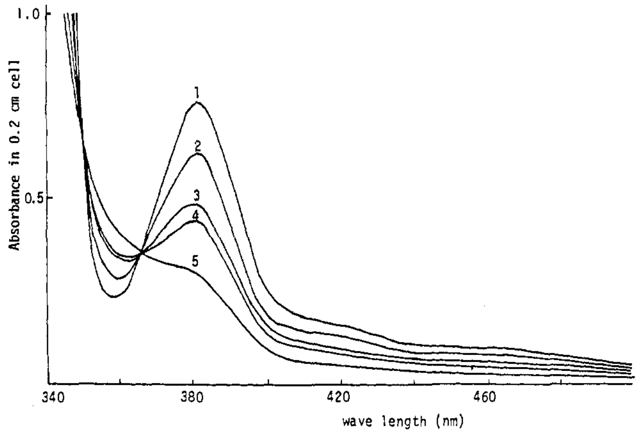

Figure 1. Electronic spectra of 3.65×10^{-3} M $Pt(PEt_3)_4$ in *n*-heptane at 20 °C with increasing concentrations of added PEt_3: (1) none, (2) 0.134 M, (3) 0.401 M, (4) 0.670 M, (5) 1.340 M.

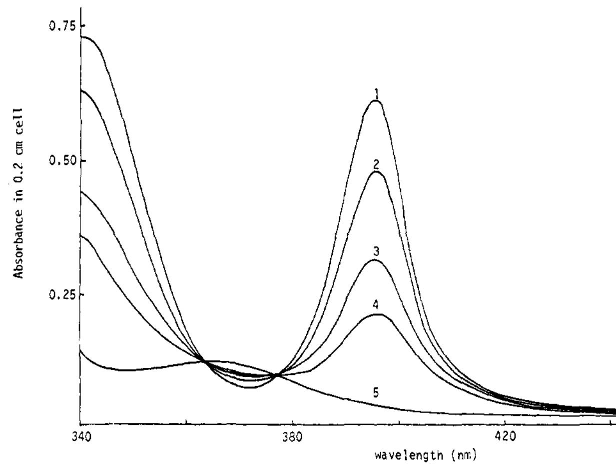

Figure 2. Electronic spectra of 2.57×10^{-3} M $Pt[P(i\text{-}Pr)_3]_3$ solution in *n*-heptane at 20 °C with increasing concentration of added $P(i\text{-}Pr)_3$: (1) none, (2) 0.030 M, (3) 0.049 M, (4) 0.099 M, (5) 0.986 M.

intensities of three parent isotope ions were 137.2 (M), 84.3 (M + 1), and 10.4 (M + 2). The *d* distribution was d_0, 59.2; d_1, 36.4; d_2, 4.5%. The percent exchange of cinnamaldehyde was 23. The corresponding value evaluated from ^1H NMR data was 25%. Employing aqueous NaOH, no H-D exchange of cinnamaldehyde was observed.

VI. *l*-Menthone. *l*-Menthone ($[\alpha]^{23}{}_D$ −27.4°) was deuterated by catalysis of $Pt(PEt_3)_3$ under similar conditions as above to give a mixture of deuterated *l*-menthone and *d*-isomenthone ($[\alpha]^{23}{}_D$ 15.2° (*c* 10.0, $CHCl_3$)) quantitatively. The corrected relative intensities of four parent isotope ions were 2.0 (M), 7.2 (M + 1), 37.2 (M + 2), and 68.1 (M + 3), suggesting the *d* distribution to be d_0, 1.7; d_1, 6.3; d_2, 32.5; d_3, 59.3%. The total exchange was 83%. A similar reaction using H_2O gave a mixture of unlabeled *l*-menthone and *d*-isomenthone, $[\alpha]^{23}{}_D$ 15.0 (*c* 11.0, $CHCl_3$); the ^1H NMR spectrum measured in the presence of Eu(*fod*)$_3$ (the ratio of optical shift reagent and the substrate being 0.36) shows the methyl proton signals of the isopropyl group of *l*-menthone and those of *d*-isomenthone at δ 2.89 (d, 2.1 H) and 2.41 (d, 0.9 H), respectively.

Kinetic Measurements. Pyridine solutions containing $Pt(PEt_3)_3$ or NaOH, D_2O, and acetophenone were prepared below −40°C and aliquots were transferred into ^1H NMR tubes. The reaction rates were measured at −10, 0, or 10 °C by following the intensity decrease of the methyl proton signal of acetophenone. Cyclohexane was employed as an internal reference of the intensity. The concentration ranges examined for catalyst, D_2O, and acetophenone were 5.4×10^{-3}–16.2×10^{-3}, 1.0–4.0, and 0.1–1.8 M, respectively.

Hydration Reactions. I. CH_3CN. A mixture of $Pt[PPh(t\text{-}Bu)_2]_2$ (37.3 mg, 0.06 mmol), CH_3CN (5 mL), and H_2O (1 mL) was heated at 80 °C for 20 h. After concentration under reduced pressure, the solid residue was sublimed to give CH_3CONH_2 (350 mg, 5.9 mmol). Extraction of the sublimation residue with *n*-hexane and subsequent evaporation gave $Pt[PPh(t\text{-}Bu)_2]_2$ (32 mg).

II. $CH_2{=}CHCN$. A mixture of $Pt(PEt_3)_3$ (22.2 mg, 0.033 mmol), $CH_2{=}CHCN$ (5 mL), and H_2O (1 mL) was heated at 80 °C for 20 h. VPC (PEG 20M, 1.5 m, 200 °C) employing naphthalene as reference showed the formation of $CH_2{=}CHCONH_2$ (30 mg, 0.42 mmol), $HOCH_2CH_2CN$ (31 mg, 0.43 mmol), $(NCCH_2CH_2)_2O$ (607 mg, 4.9 mmol), and $CH_2{=}C(CN)CH_2CH_2CN$ (50.8 mg, 0.48 mmol). Spectral data at $CH_2{=}C(CN)CH_2CH_2CN$ follow: ^1H NMR (CCl_4) δ 2.60 (m, 4 H), 5.96 (s, 1 H), and 6.05 (s, 1 H); IR (neat) 2250 (ν(C≡N)), 1620 (ν(C=C)), and 955 cm^{-1} ($\delta(H_2C{=})$); mass (calcd for $C_6H_6N_2$) *m/e* 106.

III. Crotonitrile. A mixture of $Pt(PEt_3)_3$ (67.5 mg, 0.1 mmol), $CH_3CH{=}CHCN$ (2.0 mL), and H_2O (0.5 mL) in dioxane (2.5 mL) was heated at 80 °C for 20 h. After concentration under reduced pressure, the oily residue was analyzed by VPC (PEG 20M, 1.5 m, 200 °C) and shown to contain $CH_3CH{=}CHCONH_2$ (46.7 mg, 0.54 mmol) and $CH_3CH(OH)CH_2CN$ (363 mg, 4.21 mmol).

Results and Discussion

Ligand Dissociation from $Pt(PEt_3)_4$ and PtL_3 (L = PEt_3, $P(i\text{-}Pr)_3$). Muetterties et al.[9] have shown that $Pt(PEt_3)_4$ yields $Pt(PEt_3)_3$ on heating in vacuo with dissociation of 1 mol of PEt_3. The electronic spectrum of $Pt(PEt_3)_3$ in *n*-heptane or THF exhibits a maximum at 381 nm (ϵ 1.0×10^3) and two shoulders at 420 (ϵ 1.6×10^2) and 460 nm (ϵ 1.0×10). A solution prepared by dissolving $Pt(PEt_3)_4$ in the same solvent exhibits an essentially identical spectrum. The spectra of the system $Pt(PEt_3)_4$–PEt_3 obtained with varying concentration of PEt_3 show two isosbestic points at 351 and 364 nm (Figure 1). The dissociation constants (K_L) evaluated from the spectra are 0.5 (in THF) and 0.3 M (in *n*-heptane) at 20 °C. Further dissociation of $Pt(PEt_3)_3$ to $Pt(PEt_3)_2$ is negligible since the spectrum of $Pt(PEt_3)_3$ obeys Beer's law over a wide range of concentration, 2.2×10^{-2} to 2.2×10^{-4} M.

Physical properties including ^1H NMR and molecular weight of $Pt[P(i\text{-}Pr)_3]_3$ suggest an extensive dissociation of $P(i\text{-}Pr)_3$ to give $Pt(P(i\text{-}Pr)_3]_2$.[15] The visible spectrum of $Pt[P(i\text{-}Pr)_3]_3$ in *n*-heptane shows an absorption maximum at 396 nm (ϵ 2.4×10^{-3}), no change in the molar extinction coefficient being observed over a wide range of concentration, 2.57×10^{-2} to 2.57×10^{-4} M. Incremental addition of $P(i\text{-}Pr)_3$ causes the intensity at 396 nm to decrease and a new maximum to be observed at 366 nm (Figure 2). Thus, the maxima at 396 and 366 nm may be assigned to the metal to ligand charge transfer transitions of $Pt[P(i\text{-}Pr)_3]_2$ and $Pt[P(i\text{-}Pr)_3]_3$, respectively. The assignment seems to be reasonable as the analogous transition of NiL_3(L = phosphine, phosphite) is known to occur at a longer wavelength than that of NiL_4.[22] A bathochromic shift observed on decreasing the coordination number of a d^{10} system may be explicable in terms of an increase in the energy level of the HOMO d orbital: T_{2g} (1.78 *Dq*) for Td, $d_{x^2-y^2}$ and d_{xy} (5.46 *Dq*) for trigonal planar, and d_{z^2} (10.28 *Dq*) for linear.[23]

Two isosbestic points observed at 346 and 378 nm (Figure 2) establish a simple stoichiometry for the ligand dissociation from $Pt[P(i\text{-}Pr)_3]_3$. The dissociation constant (K_L) is 4.0×10^{-2} M in *n*-heptane at 20 °C while the corresponding value in THF is 1.4×10^{-1} M, suggesting a considerable stabilization of two-coordinate complex by THF solvation. The distinct difference in ligand dissociative trends between $Pt(PEt_3)_3$ and $Pt[P(i\text{-}Pr)_3]_3$ is ascribed to the steric effect of phosphine (cone angle[24] 132 ± 4° for PEt_3, 160 ± 10° for $P(i\text{-}Pr)_3$).

Oxidative Addition of H_2O to $Pt[P(i\text{-}Pr)_3]_n$ (n = 2, 3). Water (pK_a = 15.7), being a stronger acid than MeOH (pK_a = 17.7), which shows a facile oxidative addition to PtL_n (n = 2, L = $PPh(t\text{-}Bu)_2$, $P(i\text{-}Pr)_3$, $P(c\text{-}C_6H_{11})_3$; n = 3, L = PEt_3, $P(i\text{-}Pr)_3$),[4] is expected undergo a similar addition to PtL_n. Indeed, the ^1H NMR spectrum of $Pt[P(i\text{-}Pr)_3]_3$ in the presence of a large excess of H_2O ($[H_2O]/[Pt] \simeq 300$) measured at room

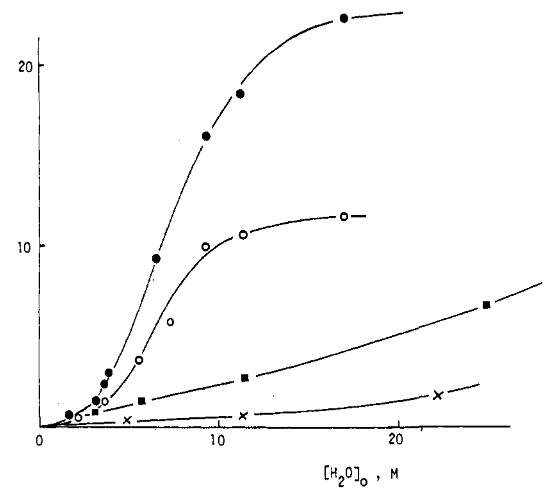

Figure 3. Dependence of equivalent conductance of $Pt[P(i\text{-}Pr)_3]_3$ (9.9×10^{-3} M) on H_2O concentration in pyridine (●, at 20 °C; ○, at 0.5 °C), acetone (■, at 20 °C), and THF (X, at 20 °C).

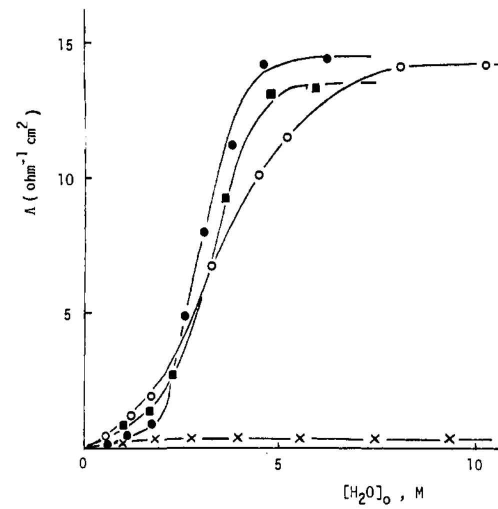

Figure 4. Dependence of equivalent conductance of $Pt(PEt_3)_3$ (9.8×10^{-3} M, ■, in pyridine; ○, in THF) and $M(PEt_3)_4$ (9.3×10^{-3} M in pyridine, ●, M = Pt; X, M = Pd, Ni) on H_2O concentrations at 0.5 °C.

temperature in pyridine exhibits a hydrido signal (δ −19.6, t, $J_{H\text{-}P}$ = 13.0, $J_{H\text{-}Pt}$ = 1064 Hz) together with signals due to two $P(i\text{-}Pr)_3$ in trans (CH_3, δ 1.08, q, $^3J_{H\text{-}P} + {}^5J_{H\text{-}P}$ = 14.4, $J_{H\text{-}P}$ = 7.2 Hz; CH, δ 2.0, m). An addition of $NaBF_4$ to the above mixture gave *trans*-$\{PtH(py)[P(i\text{-}Pr)_3]_2\}BF_4$. The result indicates that the H_2O adduct formed in pyridine must be an ion pair complex, *trans*-$\{PtH(py)[P(i\text{-}Pr)_3]_2\}OH$, which was confirmed by conductometric and pH measurements (vide infra).

The ^1H NMR spectrum of the system $Pt[P(i\text{-}Pr)_3]_2/H_2O$ ($[H_2O]/[Pt] \simeq 300$) measured in THF at room temperature also shows the formation of a H_2O adduct, *trans*-$PtH(OH)[P(i\text{-}Pr)_3]_2$ (Pt-H, δ −21.4, t, $J_{H\text{-}P}$ = 14.0, $J_{H\text{-}Pt}$ = 1012 Hz; CH_3, δ 1.24, q, $^3J_{H\text{-}P} + {}^5J_{H\text{-}P}$ = 14.0, $J_{H\text{-}H}$ = 7.0 Hz). The OH proton signal was not observed; this is perhaps due to a rapid exchange with water. An identical hydrido signal was observed for the system $Pt[P(i\text{-}Pr)_3]_3/H_2O$ in THF, no indication for the formation of either $PtH(OH)[P(i\text{-}Pr)_3]_3$ or $\{PtH[P(i\text{-}Pr)_3]_3\}OH$ being observed. It should be noted that at low H_2O concentration the system $Pt[P(i\text{-}Pr)_3]_3/H_2O$ ($[H_2O]/[Pt] \simeq 20$) shows no hydrido signal. Requirement of a large excess of H_2O for oxidative addition to $Pt[P(i\text{-}Pr)_3]_3$ to proceed suggests reversibility of the H_2O addition. Consistent with this, any attempt to isolate the H_2O adduct from the system $Pt[P(i\text{-}Pr)_3]_3/H_2O$ in THF failed, $Pt[P(i\text{-}Pr)_3]_3$ being recovered quantitatively.

We could isolate the σ-hydrido hydroxo compound *trans*-$PtH(OH)[P(i\text{-}Pr)_3]_2$ as extremely air-sensitive, colorless crystals in low yield from the system $Pt[P(i\text{-}Pr)_3]_2/H_2O$ ($[H_2O]/[Pt]$ = 370) in THF. The σ-hydrido hydroxo compound is readily soluble in saturated hydrocarbons. It is stable in aqueous THF, but slowly decomposes in dry, saturated hydrocarbons or even in solid state at room temperature under dry N_2 atmosphere. The ^1H NMR spectrum measured immediately after dissolving in benzene-d_6 shows similar signals as observed for system $Pt[P(i\text{-}Pr)_3]_2/H_2O$ in THF (Pt-H, δ −20.0, t, $J_{H\text{-}P}$ = 14.4, $J_{H\text{-}Pt}$ = 944 Hz; CH_3, δ 1.15, q, $^3J_{H\text{-}P} + {}^5J_{H\text{-}P}$ = 14.0, $J_{H\text{-}H}$ = 7.0 Hz; CH, δ 2.17, m). Note slight solvent effects on these NMR parameters, in particular those of the hydrido proton. The OH proton signal was again undetected in the region of δ −5 to 5;[10,12,25] it could be masked by the $P(i\text{-}Pr)_3$ proton signals. The presence of the OH ligand, however, was unequivocally confirmed by the IR spectrum, which shows ν_{OH} at 3600 cm^{-1}. The $\nu_{Pt\text{-}H}$ (2140 cm^{-1}) of *trans*-$PtH(OH)[P(i\text{-}Pr)_3]_2$ is considerably lower than that (2182 cm^{-1}) found in the corresponding chloride *trans*-$PtH(Cl)P(i\text{-}Pr)_3]_2$[4], suggesting a higher trans influence of OH^- than Cl^-. Recently Bennett et al.[13] have suggested that the trans influence of OH^- is comparable to that of S donors such as SPh^- on the basis of $J_{P\text{-}Pt}$ (trans) of Pt(R)(X)(diphos) (R = CH_3, C_6H_9; X = anionic ligand). These spectral data indicate considerable covalent character of the Pt-OH bond, which is rather surprising in view of the expected lack of affinity between hard OH^- and soft Pt(II).

The failure to isolate *trans*-$PtH(OH)[P(i\text{-}Pr)_3]_2$ from the system $Pt[P(i\text{-}Pr)_3]_3/H_2O$ deserves comment. For the system $PtH(OH)[P(i\text{-}Pr)_3]_3/H_2O$, the oxidative addition of H_2O seems to occur on $Pt[P(i\text{-}Pr)_3]_2$ formed by ligand dissociation rather than on the three-coordinate species $Pt[P(i\text{-}Pr)_3]_3$. The addition is reversible as shown by the stability of the H_2O adduct *trans*-$PtH(OH)[P(i\text{-}Pr)_3]_2$ in aqueous organic media and the instability in dry solvent. Therefore, the failure to isolate *trans*-$PtH(OH)[P(i\text{-}Pr)_3]_2$ from the concentrated mixture of the system $Pt[P(i\text{-}Pr)_3]_3/H_2O$ in THF is ascribed to an unfavorable equilibrium product K_LK_O (vide infra). Alternatively, reductive elimination of H_2O via intermediacy of a five-coordinate species $PtH(OH)[P(i\text{-}Pr)_3]_3$ is also possible. However, the sole hydrido hydroxo compound detected in the system $Pt[P(i\text{-}Pr)_3]_3/H_2O$ in THF by ^1H NMR spectroscopy was *trans*-$PtH(OH)[P(i\text{-}Pr)_3]_2$ and no evidence for the formation of $PtH(OH)[P(i\text{-}Pr)_3]_3$ was obtained. In addition, the latter process may be negligible for the system of low $Pt[P(i\text{-}Pr)_3]_3$ concentration as employed for the conductometric measurements (1×10^{-4} to 8×10^{-4} M).

Solution Behavior of System PtL_3/H_2O. The solution behavior of systems ML_3/H_2O was studied by conductivity and pH measurements. The conductivity of $Pt[P(i\text{-}Pr)_3]_3$ (9.5×10^{-3} M)/H_2O (0–25 M) measured in pyridine at 0.5 °C shows an anomalous dependence on H_2O concentration (Figure 3). Thus, after a slow increase, the conductivity rises abruptly above a H_2O concentration of 3.3 M ($[H_2O]/[Pt]$ ratio $\simeq$ 350). The nonlinear dependence of conductivity on $[H_2O]$ is much more clearly discernible in the $Pt(PEt_3)_3$ (9.8×10^{-3} M)/H_2O system in pyridine, which shows an inflection point around $[H_2O]$ of 1.8 M (Figure 4). Above $[H_2O]$ of 4.5 M the conductivity becomes nearly constant, its magnitude (Λ = 13.3 and 23.9 Ω^{-1} cm^2 at 0.5 and 20 °C, respectively) corresponding to a 1:1 electrolyte. The dependence on $[H_2O]$ of the conductivity of $Pt(PEt_3)_4$ (9.3×10^{-3}M)/H_2O in pyridine resembles that observed for $Pt(PEt_3)_3$ (Figure 4). In contrast to $Pt(PEt_3)_4$, $M(PEt_3)_4$ (M = Pd or Ni)/H_2O in pyridine shows extremely low conductance (Λ = 0.5 Ω^{-1} cm^2 at 0.5 °C) even

Table II. Apparent pH of System ML_n/H_2O in THF and Pyridine

	pH_{app}[a]	
	in THF[b]	in pyridine
$Pt(PEt_3)_3$	14.0	14.3
$Pt[P(i\text{-}Pr)_3]_3$	12.9	14.1
trans-$Pt(OH)(Ph)(PPh_3)_2$	8.2	14.1
NaOH	13.5	13.5

[a] [complex] = [NaOH] = 9.8×10^{-3} M. Volume ratio of H_2O vs. THF or pyridine was 2:3. Measured at 20 °C. [b] Apparent pHs of PEt_3 and $P(i\text{-}Pr)_3$ (9.8×10^{-3} M) were 9.9 and 8.6, respectively.

at a high concentration of H_2O ($[H_2O] > 5.0$ M) (Figure 4). The conductivity of the σ-hydroxo complex *trans*-$Pt(OH)(Ph)(PPh_3)_2$, which is a nonelectrolyte in dry THF, increases linearly with increase of $[H_2O]$ showing no inflection. It is worth noting that *trans*-$Pt(OH)(Ph)(PPh_3)_2$ is an electrolyte in pyridine showing a conductivity even in the complete absence of H_2O ($\Lambda = 3.8\ \Omega^{-1}\ cm^2$ at 0.5 °C) (Figure 5). Both in pyridine and THF the conductivity of *trans*-$Pt(OH)(Ph)(PPh_3)_2/H_2O$ shows a level off above $[H_2O]$ of 0.5 and 7.3 M, respectively.

The system $Pt(PEt_3)_3/H_2O$ shows a minor solvent effect for the conductivity. Thus both in pyridine and THF the conductivity shows a similar dependence on $[H_2O]$ and the magnitudes at higher water contents are nearly equal (Figure 4). This is apparently due to the absence of solvent coordination to the metal center in species $PtH(PEt_3)_3^+$. $Pt(PEt_3)_3$ is known to give an ion pair complex $PtH(PEt_3)_3^+OH^-$.[9]

A dramatic solvent effect was observed for the conductivity of the $Pt[P(i\text{-}Pr)_3]_3/H_2O$ system (Figure 3). In both acetone and THF, such an inflection as seen in pyridine is unobservable and the conductivity slowly increases almost linearly with an increase of $[H_2O]$. Furthermore the magnitude of the conductivity at the same $[H_2O]$ depends on the nature of the solvent and increases in the order THF < acetone < pyridine, a feature inexplicable in terms of the dielectric constants of solvents: THF, 7.59 (20 °C);[26] pyridine, 12.3 (25 °C);[27] acetone, 20.7 (25 °C).[27] The dissociation of one of $P(i\text{-}Pr)_3$ from $Pt[P(i\text{-}Pr)_3]_3$ was calculated from the equilibrium constant (vide supra), demonstrating that 94% of the complex ($Pt[P(i\text{-}Pr)_3]_3 = 9.8 \times 10^{-3}$ M) exists as $Pt[P(i\text{-}Pr)_3]_2$ in the absence of added phosphine in THF solution. In a coordinating solvent like pyridine the dissociation should be more extensive, although an accurate dissociation constant could not be determined.

The difference in ligand dissociative trends betwen the two phosphine complexes is also manifested in the reactions with H_2 and MeOH; $Pt[P(i\text{-}Pr)_3]_3$ gives $PtH_2[P(i\text{-}Pr)_3]_2$[4] in both reactions, while the PEt_3 analogue affords $PtH_2(PEt_3)_3$ and $[PtH(PEt_3)_3]OCH_3$,[9] respectively.

On the basis of these results the solution behavior of PtL_3 in aqueous organic solvents may be described in terms of the following equilibria 1–2 for $Pt(PEt_3)_3$ and 3–6 for $Pt[P(i\text{-}Pr)_3]_3$.

$$Pt(PEt_3)_3 + H_2O \underset{}{\overset{K_0}{\rightleftharpoons}} PtH(PEt_3)_3^+OH^- \qquad (1)$$

$$PtH(PEt_3)_3^+OH^- \overset{K_d}{\rightleftharpoons} PtH(PEt_3)_3^+ + OH^- \qquad (2)$$

The moderate solvent effect observed for $Pt(PEt_3)_3/H_2O$ (Figure 4) may be associated mainly with the dissociation of an ion-pair complex (equilibrium 2), where the dielectric constants should be influential.

In the case of $Pt[P(i\text{-}Pr)_3]_3/H_2O$, the $P(i\text{-}Pr)_3$ dissociation in strongly coordinating pyridine (equilibrium 3) should be so extensive that the main species which undergoes oxidative addition of H_2O (equilibrium 4) may be assumed to be

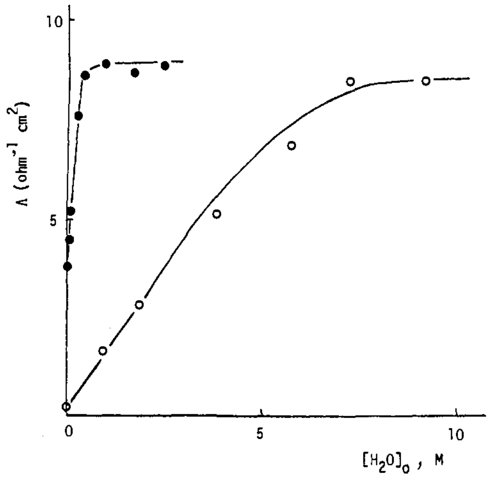

Figure 5. Dependence of equivalent conductance of *trans*-$Pt(OH)(Ph)(PPh_3)_2$ (9.80×10^{-3} M) on H_2O concentration in pyridine (●) and THF (○) at 0.5 °C.

$Pt[P(i\text{-}Pr)_3]_2$. The profound solvent effect, which is nonlinearly dependent on the dielectric constants, can be rationalized if one assumes that the coordinating power of the solvent is a determinant affecting primarily equilibrium 5. Strongly coordinating pyridine pushes the equilibrium 5 to the right in comparison with weakly coordinating acetone or THF. This view is consistent with the conductivity behaviors of *trans*-$Pt(OH)(Ph)(PPh_3)_2$ in pyridine and THF (Figure 5) which imply that the value of the product K_sK_d for the complex in anhydrous pyridine is greater than that in anhydrous THF (note that the complex is a nonelectrolyte in this solvent). In aqueous pyridine the oxidative addition (equilibrium 4) is expected to be enhanced, compared to the case in acetone or THF, owing to the solvation (equilibrium 5) and dissociation (equilibrium 6) with a favorable equilibrium product, K_sK_d.

$$PtL_3 \overset{K_L}{\rightleftharpoons} PtL_2 + L;\ L = P(i\text{-}Pr)_3 \qquad (3)$$

$$PtL_2 + H_2O \overset{K_0}{\rightleftharpoons} PtH(OH)L_2 \qquad (4)$$

$$PtH(OH)L_2 + S \overset{K_s}{\rightleftharpoons} PtH(S)L_2^+OH^- \qquad (5)$$

$$PtH(S)L_2^+OH^- \overset{K_d}{\rightleftharpoons} PtH(S)L_2^+ + OH^- \qquad (6)$$

The dissociative trend of ion-pair complexes, $PtH(PEt_3)_3^+OH^-$ and $PtH(S)[P(i\text{-}Pr)_3]_2^+OH^-$, is manifested by their apparent pHs in aqueous pyridine and THF (Table II). For comparison the apparent pH values of NaOH and *trans*-$Pt(OH)(Ph)(PPh_3)_2$ are also shown. It is remarkable that PtL_3 (L = PEt_3, $P(i\text{-}Pr)_3$) and $Pt(OH)(Ph)(PPh_3)_2$ in aqueous pyridine are stronger bases than NaOH. The apparent pH values in the two aqueous solvents observed for PtL_3 and *trans*-$Pt(OH)(Ph)(PPh_3)_2$ of course reflect their conductivity data in these solvents.

Quantitative Assessments of Equilibria Involved in PtL_3/H_2O (L = PEt_3, $P(i\text{-}Pr)_3$). The equilibria 1–2 involved in the system $Pt(PEt_3)_3/H_2O$ were treated as follows. The equilibrium constant K_0 for oxidative addition of water and the dissociation constant K_d for the ion-pair complex $PtHL_3^+OH^-$ are defined by eq 7 and 8, respectively, where f is the average activity coefficient of the free ions, $PtHL_3^+$ and OH^-. The terms in the brackets denote the concentration of PtL_3, water, and the

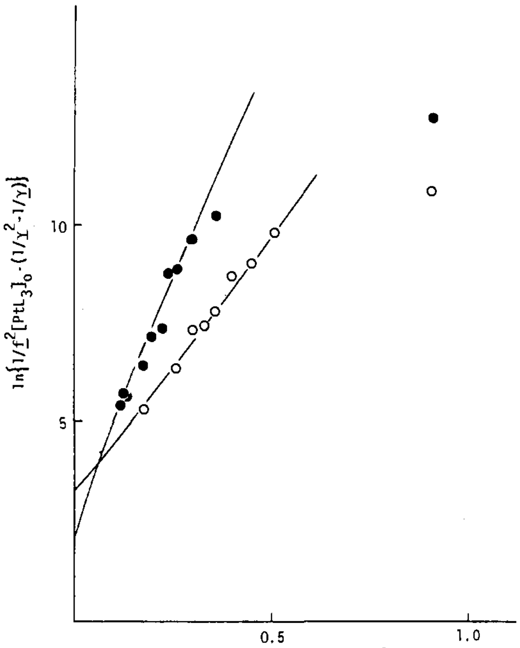

Figure 6. Plots of $\ln\{1/f^2[PtL_3]_0(1/\gamma^2 - 1/\gamma)\}$ vs. $1/[H_2O]_0$ for $Pt(PEt_3)_3$ (●) and $Pt[P(i\text{-}Pr)_3]_3$ (○). The values calculated on the basis of the equilibrium constants are shown by the lines.

ion pair complex at equilibrium, respectively.

$$K_0 = \frac{[PtHL_3{}^+OH^-]}{[PtL_3][H_2O]} \tag{7}$$

$$K_d = \frac{f^2\gamma^2[PtL_3]_0{}^2}{[PtHL_3{}^+OH^-]} \tag{8}$$

The concentration of the free ions $PtHL_3^+$ and OH^- is expressed by $\gamma[PtL_3]_0$, where γ and $[PtL_3]_0$ are free ion fraction and the initial concentration of PtL_3, respectively. The sum of the concentrations of PtL_3, $PtHL_3^+OH^-$, and $PtHL_3^+$ is equal to $[PtL_3]_0$:

$$[PtL_3]_0 = [PtL_3] + [PtHL_3{}^+OH^-] + \gamma[PtL_3]_0 \tag{9}$$

For $[H_2O]_0 \gg [PtL_3]_0$, where $[H_2O]_0$ is an initial concentration of H_2O, a combination of eq 7-9 yields

$$\frac{1}{f^2[PtL_3]_0}\left(\frac{1}{\gamma^2} - \frac{1}{\gamma}\right) = \frac{1}{K_d} + \frac{1}{K_dK_0[H_2O]_0} \tag{10}$$

The equilibria 3-6 involved in the system $Pt[P(i\text{-}Pr)_3]_3/H_2O$) were treated as follows. Since PtL_3 ($L = P(i\text{-}Pr)_3$) dissociates one of the phosphines nearly completely in dilute solution, the initial concentration of PtL_2 is approximated to be equal to that of PtL_3. The equilibrium constants for oxidative addition of H_2O to PtL_2, K_0, for ion-pair formation from $PtH(OH)L_2$, K_s, and for dissociation of the ion pair complex $PtH(S)L_2^+OH^-$, K_d, are expressed by eq 11, 12, and 13, respectively.

$$K_0 = \frac{[PtH(OH)L_2]}{[H_2O][PtL_2]} \tag{11}$$

$$K_s = \frac{[PtH(S)L_2{}^+OH^-]}{[PtH(OH)L_2]} \tag{12}$$

$$K_d = \frac{f^2\gamma^2[PtL_2]_0{}^2}{[PtH(S)L_2{}^+OH^-]} \tag{13}$$

The initial concentration $[PtL_2]_0$ is equal to the sum of the concentrations of PtL_2, $PtH(OH)L_2$, $PtH(S)L_2^+OH^-$, and $PtH(S)L_2^+$ (eq 14). The concentration of $PtH(S)L_2^+$ is given by $\gamma[PtL_2]_0$. For $[H_2O]_0 \gg [PtL_2]_0$ the rearrangement of eq 11-14 gives eq 15.

Table III. H-D Exchange of Acetophenone with D_2O[a]

catalyst	deuteration, %
trans-$Pt(OH)(Ph)L_2$[b]	62
trans-$Pt(OH)(CCl{=}CCl_2)L_2$[b]	20
trans-$Pd(OH)(CCl{=}CCl_2)L_2$[b]	12
$Pt(PPh_3)_3$	0
$Pt(PEt_3)_3$	81
$Pt[P(i\text{-}Pr)_3]_3$	86
$Pt[PPh(t\text{-}Bu)_2]_2$	3
$Pt[P(c\text{-}C_6H_{11})_3]_2$	80
$Pd[P(c\text{-}C_6H_{11})_3]_2$[c]	3
$Pd(PEt_3)_3$[c]	37
$Ni(PEt_3)_3$	14
PEt_3	0

[a] $PhCOCH_3$ (0.43 M)-D_2O (6.9 M)-catalyst (2 mM) in THF at 80 °C for 20 h. [b] $L = PPh_3$. [c] A considerable decomposition of catalyst was observed.

$$[PtL_2]_0 = [PtL_2] + [PtH(OH)L_2] + [PtH(S)L_2{}^+OH^-] + \gamma[PtL_2]_0 \tag{14}$$

$$\frac{1}{f^2[PtL_2]_0}\left(\frac{1}{\gamma^2} - \frac{1}{\gamma}\right) = \frac{1}{K_d} + \frac{1}{K_dK_s} + \frac{1}{K_dK_sK_0[H_2O]_0} \tag{15}$$

The equilibrium constants K_0, K_d, and K_s were calculated according to the Fuoss treatment[28] (see Appendix). Calculations have shown that K_d can be replaced by $K_d{}^0 \exp(-P/[H_2O]_0)$. This seems reasonable since the dissociation constant K_d of salts, e.g., n-$Bu_4N^+Br^-$, was found to be proportional to $\exp(-e^2/aDkT)$ where D is the dielectric constant of the solvent.[29] Further, a linear correlation exists between the dielectric constant of aqueous pyridine and the water content for the range of $[H_2O]_0$ examined (2.2-9.2 M). Accordingly, eq 10 and 15 are modified to eq 16 and 17, respectively.

$$\frac{1}{f^2[PtL_3]_0}\left(\frac{1}{\gamma^2} - \frac{1}{\gamma}\right) = \frac{1}{K_d{}^0 \exp(-P/[H_2O]_0)}\left(1 + \frac{1}{K_0[H_2O]_0}\right) \tag{16}$$

$$\frac{1}{f^2[PtL_2]_0}\left(\frac{1}{\gamma^2} - \frac{1}{\gamma}\right) = \frac{1}{K_d{}^0 \exp(-P/[H_2O]_0)} \times \left(1 + \frac{1}{K_s} + \frac{1}{K_0K_s[H_2O]_0}\right) = \frac{K_s + 1}{K_d{}^0K_s}\frac{1}{\exp(-P/[H_2O]_0)} \times \left(1 + \frac{1}{(K_s + 1)K_0[H_2O]_0}\right) \tag{17}$$

The equilibrium constants K_0 and $K_d{}^0$ and the proportionality constant P for the $Pt(PEt_3)_3/H_2O$ system thus assessed are 0.6 (0.3) M^{-1}, 4.2 (0.2) $\times 10^{-2}$ M, and 11.0 (0.1) M, respectively. For the $Pt[P(i\text{-}Pr)_3]_3/H_2O$ system it is impossible to assess K_0, $K_d{}^0$, and K_s separately; instead the values of composite constants, $(1 + K_s)K_0$, $K_sK_d{}^0/(1 + K_s)$, and P may be calculated from eq 17 to give 0.1 (0.06) M^{-1}, 1.2 (0.1) $\times 10^{-1}$ M, and 20.8 (0.2) M, respectively. The agreement between observed plots of $\ln\{1/f^2[PtL_3]_0(1/\gamma^2 - 1/\gamma)\}$ vs. $1/[H_2O]_0$ for the $Pt(PEt_3)_3/H_2O$ system and those calculated on the basis of K_0, $K_d{}^0$, and P values is reasonable (Figure 6). A similar plot for the $Pt[P(i\text{-}Pr)_3]_3/H_2O$ system is shown in Figure 6. Discrepancies, however, are observed in both systems at a lower water content, <2.0 ($Pt(PEt_3)_3$) and <3.5 M ($Pt[P(i\text{-}Pr)_3]_3$), where an inflection in the conductance was observed. This strongly suggests that a large excess of H_2O with respect to PtL_3 (e.g., $[H_2O]/[Pt(PEt_3)_3] > 200$) is required for it to undergo oxidative addition. This may be ascribed to the highly hydrophobic nature of PtL_3 which prevents the approach of a H_2O molecule. Consistent with this, the conductance of *trans*-$Pt(OH)(Ph)(PPh_3)_2/H_2O$ in pyridine

Table IV. H-D Exchange Reaction of Carbonyl Compounds by $Pt(PEt_3)_3$[a]

	d distribution, %							
	d_0	d_1	d_2	d_3	d_4	d_5	H atom exchangeable[b]	deuteration, %
acetophenone	3.4	17.4	37.1	42.1			PhCOC*H*$_3$	72
cyclohexanone	3.2	12.5	31.2	36.9	16.3		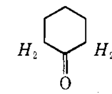	63
propiophenone	5.7	30.9	63.4				PhCOC*H*$_2$CH$_3$	79
l-menthone	1.7	6.3	32.5	59.5			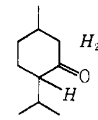	83
(*S*)-(+)-methyldeoxybenzoin	41.9	58.1					PhCOC*H*(CH$_3$)Ph	58
d-camphor	7.2	34.3	58.5				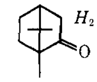	76
nopinone	5.9	27.3	63.2	3.6			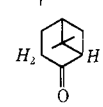	55
phenyl propenyl ketone	31.6	45.7	16.7	5.5	0.5		PhCOC*H*=CHC*H*$_3$	24
benzalacetone	6.8	19.1	31.4	28.9	13.8		PhCH=C*H*COC*H*$_3$	56
l-carvone	4.7	35.4	52.6	7.3			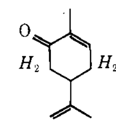	54
cinnamaldehyde	75.9	36.4	4.5				PhCH=C*H*CH*O*	23
progesterone[c]	0.3	0.7	3.0	9.1	18.4	25.8[d]	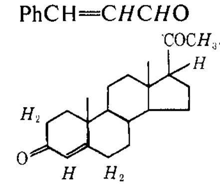	58
testosterone propionate	18.3	36.8	23.6	13.1	7.7	0.5	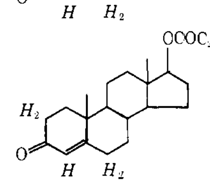	31

[a] Substrates (2 M)-D_2O (10 M)-$Pt(PEt_3)_3$ (15 mM) in THF at 80 °C for 20 h. [b] H atom exchangeable is shown by *H*. [c] D distribution catalyzed by aqueous NaOH: d_0, 60.6; d_1, 27.9; d_2, 8.8; d_3, 1.9; d_4, 0.8. [d] d_6, 23.7; d_7, 14.0; d_8, 4.5; d_9, 0.6.

steadily increases without inflection as the water content increases (Figure 5).

Comparison of the K_0 value of the $Pt(PEt_3)_3/H_2O$ system with the $(1 + K_s)K_0$ value for the $Pt[P(i\text{-}Pr)_3]_3/H_2O$ system suggests that oxidative addition of H_2O to the three-coordinate $Pt(PEt_3)_3$ is favored as compared to the two-coordinate complex $Pt[P(i\text{-}Pr)_3]_2$. This is understandable. Firstly, the basicity of the two phosphines being roughly comparable,[30] a higher metal basicity is expected for the three-coordinate complex with respect to the two-coordinate complex. Secondly, an enhanced stability of the ion-pair complex $PtH(PEt_3)_3^+OH^-$ toward reductive elimination of H_2O, compared to σ-hydrido hydroxo complex *trans*-$PtH(OH)[P(i\text{-}Pr)_3]_2$, is expected from steric considerations.

H-D Exchange of the Activated C-H Bond with D_2O. Since hydrido hydroxo complexes derived from oxidative addition of H_2O to $Pt(PR_3)_n$ appear to be stronger bases than aqueous alkali in organic media, they should be able to serve as substitutes for conventional alkali bases. Firstly we examine the effectiveness for H-D exchange reactions of activated C-H bonds.

Treatment of $PhCOCH_3$ with a large excess of D_2O (1:16) in the presence of a catalytic amount of $Pt[P(i\text{-}Pr)_3]_3$ at 80 °C for 20 h in THF gave methyl-deuterated acetophenone; the deuteration reaches 86%, as determined by mass and ^1H NMR spectra. Remarkably, $Pt(PEt_3)_3$ proved to be a catalyst more active than aqueous NaOH. The rate constants, K_{obsd} (M^{-1} s^{-1} at −10 °C), for $Pt(PEt_3)_3$ and NaOH are 6.4×10^{-2} and 2.4×10^{-2} respectively (vide infra). The catalytic activity of zerovalent complexes of the nickel triad (Table III) depends on the phosphine ligands and on the metal. The activity increases in the sequence $PPh_3 < PPh(t\text{-}Bu)_2 \ll P(c\text{-}C_6H_{11})_3 \simeq PEt_3 < P(i\text{-}Pr)_3$. The triphenylphosphine complex $Pt(PPh_3)_3$ is totally inactive. The trend can be interpreted by a composite of steric and electronic properties of the phosphine ligands. The effect of the metal center can be compared for the nickel triad complexes $M(PEt_3)_3$; the activity decreases in the order Pt > Pd > Ni. Hydroxo complexes containing PPh_3 as an auxiliary ligand, e.g., *trans*-$M(OH)(R)(PPh_3)_2$[12] (M = Pd, R = $CCl{=}CCl_2$; M = Pt, R = $CCl{=}CCl_2$, Ph), show catalytic activity which depends on the σ-bonded organic moiety in the trans position; the σ-phenyl complex is more active than the $CCl{=}CCl_2$ analogue.

The scope of organic compounds which undergo the catalytic H-D exchange was studied employing the $Pt(PEt_3)_3/H_2O$ system. The following ketones were examined: cyclohexanone, propiophenone, *d*-camphor, nopinone, *l*-menthone, and (*S*)-(+)-methyldeoxybenzoin (Table IV). The H-D exchange

Table V. H-D Exchange Reaction of Sulfoxide, Sulfone, and Nitroalkane by $Pt(PEt_3)_3$[a]

	d distribution, %							H atom exchangeable[b]	deuteration, %
	d_0	d_1	d_2	d_3	d_4	d_5	d_6		
dimethyl sulfoxide	1.2	6.5	18.2	30.2	27.4	14.0	2.5	CH_3SOCH_3	54
methyl ethyl sulfoxide	4.5	24.6	41.0	24.3	2.1	3.5		$CH_3SOCH_2CH_3$	41
dimethyl sulfone	0.8	3.7	11.9	26.0	31.7	21.1	4.8	$CH_3SO_2CH_3$	61
nitromethane	18.6	29.1	32.7	19.6				CH_3NO_2	51

[a] Substrates (2 M)-D_2O (10 M)-$Pt(PEt_3)_3$ (15 mM) in THF at 80 °C for 20 h. [b] H atom exchangeable is shown by *H*.

takes place selectively at the α position and no deuterium incorporation at the β position was observed, For *d*-camphor, both axial and equatorial hydrogens are equally deuterated and no selection occurs between the sterically less hindered equatorial and hindered axial hydrogen atoms, Remarkably, a bridgehead hydrogen in nopinone, which does not enter in the keto-enol tautomerism, is deuterated.

Since one of the hydrogens in *l*-menthone to be deuterated is attached to the chiral carbon (C_4), its H-D exchange may afford information on the mechanism. The specific optical rotation of menthone obtained from the reaction of *l*-menthone with H_2O catalyzed by $Pt(PEt_3)_3$ at 80 °C for 20 h was $[\alpha]^{23}{}_D$ 15.0°. The corresponding value of *l*-menthone is $[\alpha]^{23}{}_D$ −27.4°. The ratio of *l*-menthone and *d*-isomenthone in the

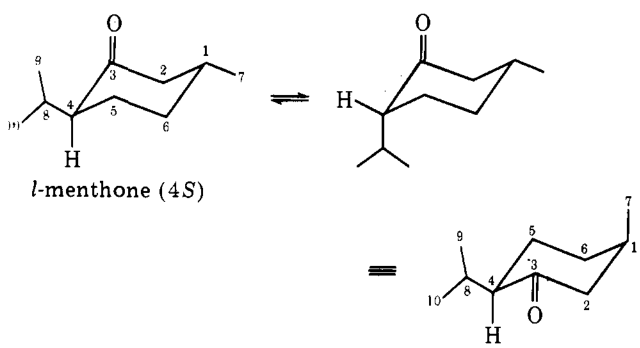

l-menthone (4*S*)

d-isomenthone (4*R*)

reaction products are 1:0.46, as determined from the relative intensity of the isopropyl protons' signals (see Experimental Section). The ratio is comparable to the thermal equilibrium ratio (1:0.43 at 25 °C).[31] Since an asymmetric induction at C_4 by another chiral carbon (C_1) is possible, this result alone provides no clue for the mechanism. Therefore, (*S*)-(+)-methyldeoxybenzoin[20] ($[\alpha]^{21}{}_D$ 54°; optical purity 27%) with one chiral carbon was examined. A complete loss of optical activity was found. Thus the H-D exchange by the catalysis of $Pt(PEt_3)_3$ takes place without retention of the carbon configuration. However, this result does not exclude a concerted mechanism. Inversion at the chiral carbon atom should result in a loss of optical activity, because of the reversibility of the H-D exchange reaction.

The $Pt(PEt_3)_3$-catalyzed reaction of lower alkylaldehydes, e.g., *n*-butyraldehyde, with D_2O was always accompanied by polymerization, presumably via aldol condensations. Capronaldehyde and β-phenylpropionaldehyde give deuterated aldehydes in low yield (10 and 4%, respectively) together with intractable aldol condensation products. The ^1H NMR analyses show deuterium incorporation at the aldehydic proton as well as the α-methylene group, which cannot be effected by alkaline hydroxide. For capronaldehyde the deuterations at α-CH_2 and CHO are 58 and 66%, respectively. The corresponding values for β-phenylpropionaldehyde are 39 and 10%. In contrast to alkylaldehydes, no H-D exchange of the aldehydic proton was observed for benzaldehyde, furfural, and DMF. However, deuterium incorporation at the aldehydic proton occurs for α, β-unsaturated aldehydes.

Remarkably, in α,β-unsaturated carbonyl compounds, e.g., phenyl propenyl ketone, benzalacetone, and cinnamaldehyde, both α-olefinic and allylic protons are deuterated (Table IV). Crotonaldehyde gave only polymerizates. In no case was deuteration at the β-olefinic position observed. Aqueous NaOH does not catalyze the H-D exchange of allylic and α-olefinic protons nor of an aldehydic proton. The conventional η^2 coordination of the olefinic bond to a metal center would lead to the exchange of both α- and β-CH bonds. The activa-

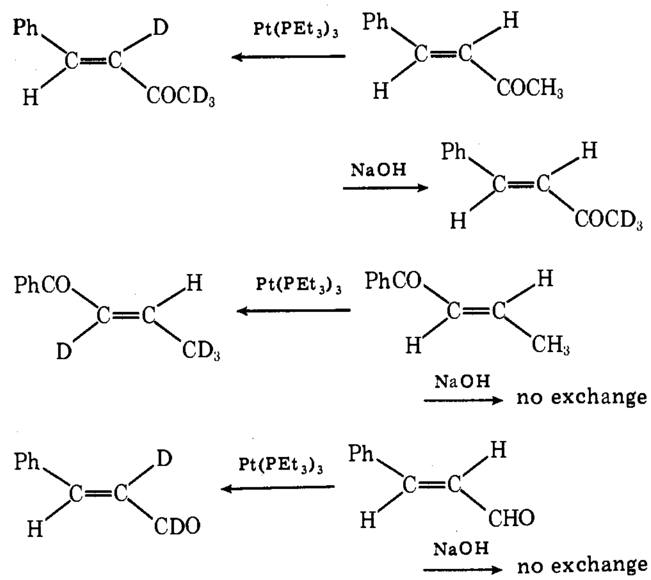

tion of the α-CH bond could occur via an intermediate η^3-oxoallyl species, as this type of bonding is seen in $[(\eta^3\text{-RCOCHCl})PdCl]_2$ (R = Ph, CH_3)[32] and $\{[\eta^3\text{-}o\text{-OC(Me)-(CMe)}]C_6H_4PPh_2\}Mn(CO)_3$.[33] The deuterations of α-CH_3 and α-olefinic protons of benzalacetone estimated by ^1H NMR are 56 and 64%. The corresponding values for the allylic and α-olefinic protons of phenyl propenyl ketone are 34 and 82%. Qualitatively the exchange rate increases in the sequence allylic hydrogens < α-olefinic hydrogen < α-methyl hydrogens.

The H-D exchange of the active α-CH bond in sulfones, sulfoxides, and nitroalkanes is also effected by $Pt(PEt_3)_3$ (Table V). It has been shown that both methyl and aromatic hydrogens in toluene are deuterated by D_2O via catalysis with $PtCl_4{}^{2-}/DCl$.[34] The $Pt(PEt_3)_3/D_2O$ system fails to catalyze the H-D exchange of toluene and diphenylmethane. However, the H-D exchange of methine, methylene, or olefinic protons in triphenylmethane, fluorene, and indene occurs with the present catalyst system (Table VI). Obviously a correlation exists between the pK_a of the aromatic substrates and the exchanged rate. Thus the deuterium incorporation increases in the order diphenylmethane ≪ triphenylmethane < fluorene < indene.

An interesting application of the ML_n/H_2O system may be the H-D exchange for elaborate compounds such as hormones. Thus, testosterone propionate and progesterone are deuterated at α-olefinic and allylic as well as α-aliphatic carbons (Table IV). Aqueous NaOH is less efficient for the H-D exchange of progesterone. The *d* distribution is d_0, 60.6; d_1, 27.9; d_2, 8.8;

Table VI. H-D Exchange Reaction of Hydrocarbons by $Pt(PEt_3)_3$[a]

	d distribution, %				H atom exchangeable[b]	deuteration, %	pK_a
	d_0	d_1	d_2	d_3			
diphenylmethane	100					0	35
triphenylmethane	95.0	5.0			Ph_3CH	5	33
fluorene	23.5	42.3	34.2		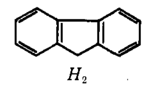	55	25
indene	11.8	29.9	24.8	33.5	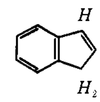	60	21

[a] Substrates (2 M)-D_2O (10 M)-$Pt(PEt_3)_3$ (15 mM) in THF at 80 °C for 20 h. [b] H atom exchangeable is shown by *H*.

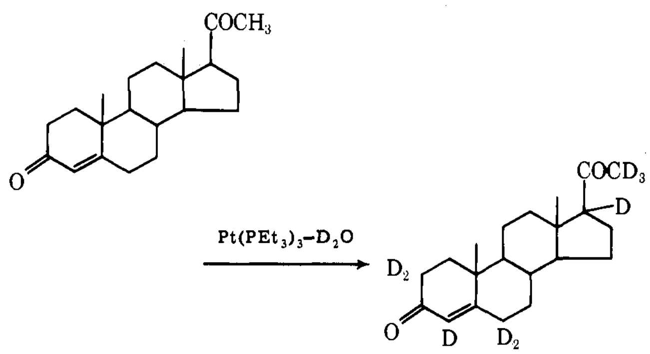

d_3, 1.9; d_4, 0.8. No deuterium incorporation is observed at α-olefinic hydrogen.

Kinetics of the $Pt(PEt_3)_3$-catalyzed H-D exchange reaction of $PhCOCH_3$ with D_2O in pyridine were studied by measuring the increase of intensity of the H_2O proton signal and/or the decrease of the methyl proton signal of $PhCOCH_3$. The rate exhibits first-order kinetics with respect to the concentrations of $Pt(PEt_3)_3$ and $PhCOCH_3$. Below 1.76 M H_2O concentration the H-D exchange reaction virtually does not take place, while the rate is almost independent of H_2O concentration for the range 1.98-3.90 M. At first sight this appears to be incompatible with the conductivity behavior which shows a sharp increase in conductance for the same range of H_2O concentration. The independence of the rate of H_2O concentration implies the unimportance of free OH^- ion in the rate-determining step of the catalysis. This is also manifested by the fact that the relative catalytic reactivities in THF, $Pt(PEt_3)_3 < Pt[P(i\text{-}Pr)_3]_3$, are the reverse of the apparent pH values, $Pt(PEt_3)_3 > Pt[P(i\text{-}Pr)_3]_3$. The rate dependence on the complex strongly suggests the active species participating in the rate-determining step to be the ion-pair complex $PtH(PEt_3)_3^+OH^-$. The concentration of the ion-pair complex is expressed by $K_0[H_2O]/(1 + K_0[H_2O])$ ($K_0 = 0.6\ (0.3)\ M^{-1}$) and is virtually independent of H_2O concentration for the range examined. The rate is expressed by $R = k[Pt(PEt_3)_3][PhCOCH_3]$ and the activation parameters obtained from the rate constants (Table VII) are $\Delta H^{\ddagger}_{273} = 6.0 \pm 1.6$ kcal mol^{-1} and $\Delta S^{\ddagger}_{273} = -42.7 \pm 5.7$ eu.

Recently a novel condensation reaction of hydroxo complexes with compounds containing activated C-H bond has been reported.[3,11-13] The reverse reaction, hydrolysis of the σ-alkyl complex to regenerate a hydroxo complex and alkane, also takes place readily. Thus, gentle heating of *trans*-$Pt(CH_2COPh)(Ph)(PPh_3)_2$ with an excess of H_2O in THF gave *trans*-$Pt(OH)(Ph)(PPh_3)_2$. The phenyl group remains intact, suggesting a facile hydrolysis of the more polar Pt-CH_2COPh bond[35] rather than Pt-Ph. It is likely then that the H-D exchange reaction of $PhCOCH_3$ catalyzed by *trans*-$Pt(OH)(Ph)(PPh_3)_2$ proceeds through a reversible condensation reaction.

Table VII. Rate Constants for the H-D exchange of $PhCOCH_3$[a]

temp, K	k, $s^{-1}\,M^{-1}$
263	0.64×10^{-1}
273	1.17×10^{-1}
283	1.44×10^{-1}

[a] $Pt(PEt_3)_3$ 8.1×10^{-3} M, $PhCOCH_3$ 0.145 M, and D_2O 1.98 M in pyridine.

$$trans\text{-}Pt(OD)(Ph)(PPh_3)_2 \underset{PhCOCH_2D \quad D_2O}{\overset{PhCOCH_3 \quad HDO}{\rightleftharpoons}} trans\text{-}Pt(CH_2COPh)(Ph)(PPh_3)_2$$

Based on these results we suggest that the first step in the H-D exchange of $PhCOCH_3$ catalyzed by $Pt(PEt_3)_3$ involves reversible oxidative addition of D_2O to $Pt(PEt_3)_3$ to give $PtD(PEt_3)_3^+OD^-$ (equilibrium 1). Condensation with $PhCOCH_3$ will follow producing the deuterido benzoylmethyl complex $PtD(CH_2COPh)(PEt_3)_3$ with liberation of DHO (equilibrium 18). The final step, affording the methyl-deuterated acetophenone, may involve either hydrolysis (step 19) or reductive elimination (step 20). For the reaction catalyzed by *trans*-$M(OH)(R)(PPh_3)_2$ (M = Pd, R = $CCl{=}CCl_2$; M = Pt, R = $CCl{=}CCl_2$, Ph), step 20 can be excluded.

$$Pt(PEt_3)_3 + D_2O \rightleftharpoons PtD(PEt_3)_3^+OD^- \qquad (1)$$

$$PtD(PEt_3)_3^+OD^- + PhCOCH_3 \rightleftharpoons PtD(CH_2COPh)(PEt_3)_3 + DHO \qquad (18)$$

$$PtD(CH_2COPh)(PEt_3)_3 + D_2O \rightleftharpoons PtD(PEt_3)_3^+OD^- + PhCOCH_2D \qquad (19)$$

$$PtD(CH_2COPh)(PEt_3)_3 \rightarrow Pt(PEt_3)_3 + PhCOCH_2D \qquad (20)$$

The independence of the exchange rate on D_2O concentration suggests that the hydrolysis (step 19) is not the rate-determining step. Similarly the negative activation entropy is incompatible with a scheme involving the reductive elimination (step 20) as the rate-determining step. Therefore the rate-determining step could be the condensation reaction (equilibrium 18). This postulate is supported by the following observations. (1) The rate of the exchange is determined primarily by the acidity of the hydrogen atom (Table VI). (2) The catalytic activity of *trans*-$Pt(OH)(R)(PPh_3)_2$ depends on the trans-R ligand and increases in the order $CCl{=}CCl_2 <$ Ph.

Hydration of Nitriles and Olefins. Reactions of CH_3CN and H_2O in the presence of a catalytic amount of $Pt[PPh(t\text{-}Bu)_2]_2$ at 80 °C for 20 h gave 99 mol of acetamide per mol of the

Table VIII. Catalytic Hydration of Nitriles[a]

	CH_3CN →	$CH_2{=}CHCN$ →					$CH_3CH{=}CHCN$ →		
catalyst[b]	CH_3CONH_2[c]	$CH_2{=}CHCONH_2$[c]	$HOCH_2CH_2CN$[c]	$(NCCH_2CH_2)_2O$[c]	$CH_2{=}C(CN)CH_2CH_2CN$[c]	olefin/CN[d]	$CH_3CH{=}CHCONH_2$[c]	$CH_3CH(OH)CH_2CN$[c]	olefin/CN[d]
trans-$Pt(OH)(CCl{=}CCl_2)L_2$	15	9.9	tr	1.2	0.4	0.12			
trans-$Pt(OH)(CH{=}CCl_2)L_2$	18	17.4	tr	3.5	0.7	0.20			
trans-$Pt(OH)(Ph)L_2$	77	106	11.6	74.1	15.6	0.81			
PtL_3		tr	tr	3.5	0				
$Pt[P(c\text{-}C_6H_{11})_3]_2$	520	21.0	24.5	186	98.7	10.0			
$Pt[PPh(t\text{-}Bu)_2]_2$	99	7.0	31.0	201	71.7	33.0	19.0	2.5	0.13
$Pt[P(i\text{-}Pr)_3]_3$	405	36.0	49.0	418	52.5	13.0	68.0	14.0	0.21
$Pt(PEt_3)_3$	54	12.7	13.1	147	7.2	12.6	5.4	42.0	8.0
NaOH	7.5	22.3	tr	0.5	0	0.02			

[a] A mixture of complex (0.03–0.1 mmol), nitrile (5 mL), and H_2O (1 mL) was at 80 °C for 20 h. [b] L = PPh_3. [c] Mol/mol catalyst. [d] Ratio of hydration product of olefinic to C≡N group.

Scheme I. Proposed Mechanism for Nitrile Hydration

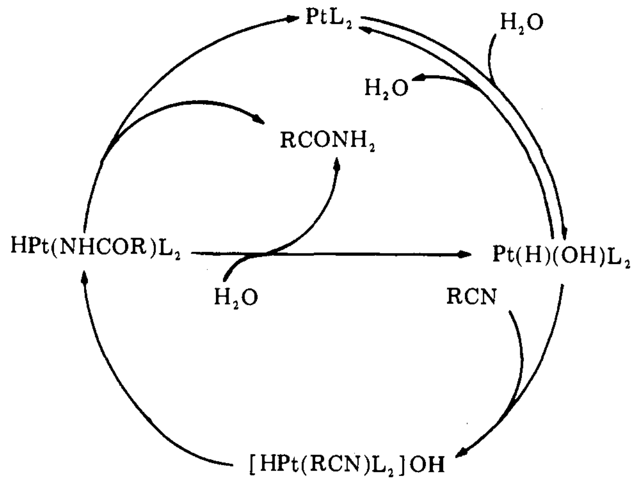

Scheme II. Proposed Mechanism for Olefin Hydration

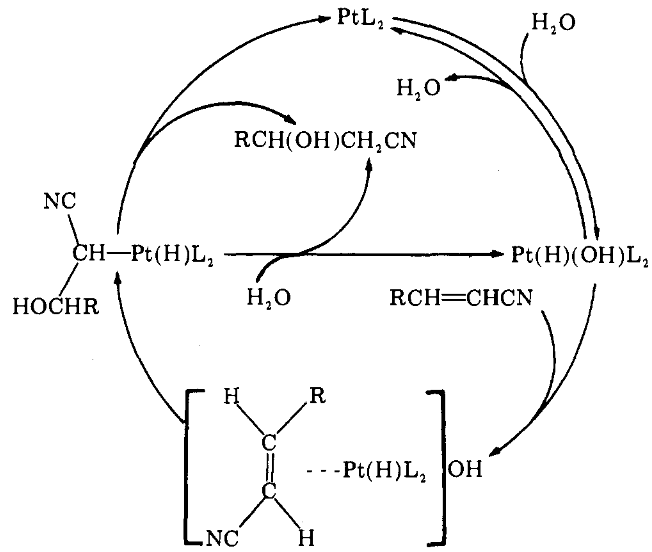

catalyst with almost complete recovery of $Pt[PPh(t\text{-}Bu)_2]_2$. The Pt(0) complexes coordinated with electron-donating phosphines, $Pt[P(i\text{-}Pr)_3]_3$ and $Pt[P(c\text{-}C_6H_{11})_3]_2$, are more efficient catalysts than those with $Pt[PPh(t\text{-}Bu)_2]_2$ (Table VIII). Similarly the hydroxo complexes, *trans*-$Pt(OH)(R)(PPh_3)_2$ (R = $CCl{=}CCl_2$, $CH{=}CCl_2$, and Ph) show catalytic activity for the hydration of nitriles. They are not, however, as efficient as compared to the coordinatively unsaturated Pt(0) complexes described above.

The Pt(0) complex-catalyzed hydration of $CH_2{=}CHCN$ gives β-hydroxypropionitrile and β,β-dicyanoethyl ether which may be derived from cyanoethylation of β-hydroxypropionitrile. An acrylonitrile dimer, $CH_2C(CN)CH_2CH_2CN$, was also formed. Hydration of $CH_3CH{=}CHCN$ effected by the Pt(0) complexes gave crotonamide and β-hydroxybutyronitrile; no crotonitrile dimer was formed. Compared to the hydration of $CH_2{=}CHCN$, the alcohol formation is drastically reduced when $Pt[PPh(t\text{-}Bu)_2]_2$ or $Pt[P(i\text{-}Pr)_3]_3$ is used. As shown in Table VIII $Pt(PEt_3)_3$ seems to be effective for the hydration of the olefinic bond. In contrast to the Pt(0) complexes, aqueous NaOH is extremely inefficient for hydration of the olefinic group. It is worth noting that an oxidation takes place in the reaction of $CH_2{=}CHCN$ with H_2O in the presence of an equimolar amount of $PdCl_2$ affording CH_3COCN.[36]

The hydration of nitriles by ML_2 catalysis probably proceeds via insertion of RCN into the Pt-OH bond or nucleophilic attack of OH^- at the N-coordinated nitrile, affording a σ-amido complex $PtH(NHCOR)L_2$. The former reaction scheme has been proposed for nitrile hydration by $Pt(OH)(C_6H_9)$(diphos) (C_6H_9 = cyclohexenyl).[37] Based on the solution behavior of the Pt(0) complexes and *trans*-$Pt(OH)(R)(PPh_3)_2$, we propose the latter mechanism to be more probable. Tentatively the hydration is described by Scheme I.

In the hydration of $CH_2{=}CHCN$ catalyzed by *trans*-$Pt(OH)(R)(PPh_3)_2$, both the olefin and nitrile hydrations increase in the order $CCl{=}CCl_2 < CH{=}CCl_2 <$ Ph. The ratio of olefin to nitrile hydration also increases in this order. Several aspects are pertinent to the discussion of the mechanism. Ligands having strong trans influence place high electron density on the metal[38] for which η^2-coordination of an olefin may be preferred, rather than the σ-type coordination of the nitrogen atom of nitrile. This view receives support from the drastic reduction in the olefin hydration of $CH_3CH{=}CHCN$ catalyzed by $Pt[P(i\text{-}Pr)_3]_3$ or $Pt[PPh(t\text{-}Bu)_2]_2$. The steric bulk of these phosphines and the methyl substituent render the η^2 coordination of $CH_3CH{=}CHCN$ much more unfavorable than for the case of $CH_2{=}CHCN$. Consistently the less bulky PEt_3 complex shows little difference between the two olefins. Thus it seems that the olefin hydration requires the η^2 coordination while the nitrile hydration demands σ-N coordination of the nitrile group. As shown in Scheme II, the olefin coordination will be accompanied by the formation of the ion-pair complex where a nucleophilic attack of OH^- will produce the σ-$HOCHRCH(CN)$-Pt moiety (R = H, CH_3). An alternative mechanism is the insertion of the olefin into the Pt-H bond.

Scheme III. Proposed Mechanism for $CH_2{=}CHCN$ Dimerization

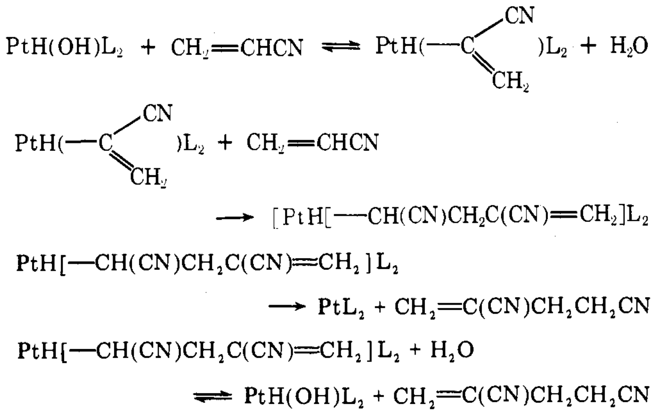

This possibility is readily excluded because the hydride ligand should attack the β-carbon atom leading to α-hydroxypropionitrile, which was not detected. The subsequent hydrolysis of σ-HOCHRCH(CN)-Pt will give $HOCHRCH_2CN$. The catalytic cycle is thus completed. Alternatively, the reductive elimination of $HOCHRCH_2CN$ is possible. However, this process can be ruled out at least for *trans*-$Pt(OH)(R)(PPh_3)_2$ by the same argument described for the H-D exchange mechanism. The extension of this catalysis to other olefins was fruitless; owing to the strong basicity of the present system, PtL_n/H_2O, polymerization was observed for methyl acrylate and methyl vinyl ketone. Alkenes, such as cyclohexene, were inert.

The observed dimerization of $CH_2{=}CHCN$ deserves comment. In view of the facile deuterium incorporation at the α position of the α,β-unsaturated bond, we propose, tentatively, a reaction scheme involving the formation of a σ-vinyl intermediate, $HPt[C(CN){=}CH_2]L_2$, through a condensation reaction (Scheme III).

A process involving an insertion of $CH_2{=}CHCN$ into the Pt-H bond is readily excluded by the efficiency of *trans*-$Pt(OH)(Ph)(PPh_3)_2$ and by the inefficiency of $\{$*trans*-$PtH(py)[P(i\text{-}Pr)_3]_2\}BF_4$ as a catalyst for dimerization of $CH_2{=}CHCN$.

Acknowledgment. This work was partially supported by the Toray Science Foundation.

Appendix

Using the Onsager relation $\Lambda = \gamma(\Lambda_0 - S\sqrt{\gamma[PtL_3]_0})$ and the Debye–Hückel equation $-\ln f = \beta''\sqrt{\gamma[PtL_3]_0}/(1 + \kappa a\sqrt{\gamma})$, values of γ and f in eq 10 and 15 were calculated by computer iteration procedure, according to the Fuoss treatment.[28] The term $\kappa a\sqrt{\gamma}$ in the Debye–Hückel equation was neglected assuming that $\kappa a\sqrt{\gamma} \ll 1$. This assumption seems to be acceptable as the dissociation constant K and Λ_0 of LiCl were found to be virtually independent over a wide range of the a value (0–10 Å).[40] The Onsager coefficient S $(= \alpha\Lambda_0 + \beta)$ is calculated by employing the dielectric constants and viscosity data[41] of aqueous pyridine at 0.5 °C. The dielectric constants of aqueous pyridine with varying water concentration (shown in parentheses) measured at 0.5°C by a transformer bridge assembly were 16.8 (2.225), 17.7 (2.775), 19.2 (3.497), 19.9 (3.886), 21.4 (4.606), 22.4 (4.995), 23.8 (5.549), 24.2 (5.741), and 33.3 (9.208). The coefficient β'' was also assessed by employing the above dielectric constants.

Since $\gamma = \Lambda/\Lambda_0 F(z)$[28] where z is $(S/\Lambda_0^{3/2})([PtL_3]_0\Lambda)^{1/2}$, eq 10 and 15 can be transformed into

$$F/\Lambda = 1/\Lambda_0 + (K/\Lambda_0^2)([PtL_3]_0\Lambda f^2/F) \qquad (21)$$

which is identical with the Fuoss equation,[28] where K is equal to $1/K_d + 1/K_dK_0[H_2O]_0$ for $Pt(PEt_3)_3$ and $1/K_d + 1/k_dK_s + 1/K_dK_sK_0[H_2O]_0$ for $Pt[P(i\text{-}Pr)_3]_3$.

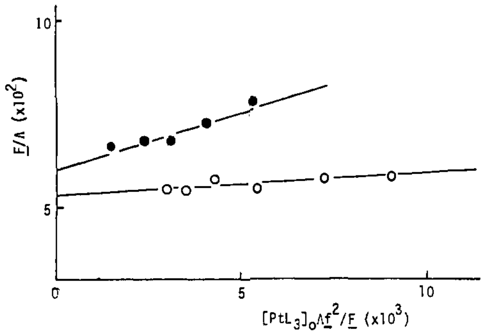

Figure 7. Conductance vs. concentration data treated according to Fuoss (eq 21) for PtL_3 (L = PEt_3, O; L = $P(i\text{-}Pr)_3$, ●) in a H_2O–pyridine mixture ($[H_2O]_0$ = 5.549 M) at 0.5 °C, PtL_3 concentration being in the range of 2×10^{-4} to 8×10^{-4} M (L = PEt_3) and 1×10^{-4} to 5.9×10^{-4} M (L = $P(i\text{-}Pr)_3$).

An initial assessment of the equivalent conductance at infinite dilution (Λ_0) in aqueous pyridine ($[H_2O]$ = 5.549 M) was derived from the intercept by extrapolation of Λ vs. $\sqrt{[PtL_3]_0}$ plots, and computer iteration procedure was employed to give the best least-squares fit of the data to the Fuoss conductance equation[28] (eq 21). The values obtained in the last iteration are plotted in Figure 7. The values of Λ_0 (Ω^{-1} cm^2) thus evaluated from the intercept of eq 21 are 18.9 (0.5) for $Pt(PEt_3)_3$ and 16.6 (0.5) for $Pt[P(i\text{-}Pr)_3]_3$ in aqueous pyridine ($[H_2O]$ = 5.549 M), the standard deviation being shown in the parentheses. The corresponding value of $Pt(PEt_3)_3$ in aqueous pyridine at $[H_2O]$ of 3.885 M is 21.8 (1.7) Ω^{-1} cm^2. The values of Λ_0 for the other $[H_2O]$ (0.550–5.549 M for $Pt(PEt_3)_3$ and 1.110–8.324 M for $Pt[P(i\text{-}Pr)_3]_3$) were assessed from Walden's rule,[42,43] $\Lambda_0\eta$ = const, where η is the viscosity of aqueous pyridine at 0.5 °C.[41] The validity of Walden's rule for the solution of $Pt(PEt_3)_3$ has been confirmed; a Walden product of 0.459 calculated by employing a Λ_0 value at $[H_2O]$ of 5.549 M (η = 2.43 cP) agrees well with that (0.443) obtained from the experimentally determined value of Λ_0 at $[H_2O]$ of 3.885 M (η = 2.03 cP).

Equation 10 was examined by plotting the left-hand side vs. $1/[H_2O]_0$. The plot does not give the expected linear correlation. However, a nearly linear correlation was observed between $\ln [1/(f^2[PtL_3]_0)(1/\gamma^2 - 1/\gamma)]$ and $1/[H_2O]_0$, suggesting that K_d is proportional to $\exp(-P/[H_2O]_0)$. Equation 10 is then modified to 16 (see text) or to its logarithmic form (22) using proportionality constants K_d^0 and P.

$$\ln\left[\frac{1}{f^2[PtL_3]_0}\left(\frac{1}{\gamma^2} - \frac{1}{\gamma}\right)\right] = \ln(1/K_d^0) + P/[H_2O]_0 + \ln\left(1 + \frac{1}{K_0[H_2O]_0}\right) \qquad (22)$$

The values of K_0, K_d^0, and P are calculated by the following procedure. Assuming $K_0[H_2O]_0 \gg 1$, the values of K_d^0 and P are obtained from the intercept and the slope of eq 22, respectively. Employing the values K_d^0 and P thus obtained, the value of K_0 was assessed from eq 22. By repeating this procedure the values of K_0, K_d^0, and P at higher order approximation were obtained. Further refinements were made by standard nonlinear three-parameter least-squares calculations.

Similarly eq 15 for $Pt[P(i\text{-}Pr)_3]_3$ is represented by eq 17 or by its logarithmic form (23). Note that eq 23 is equivalent to eq 22. The values $(K_s + 1)/K_d^0K_s$, P, and $1/k_0(K_s + 1)$ can be calculated by the same procedure employed for $Pt(PEt_3)_3$.

$$\ln\left[\frac{1}{f^2[PtL_2]_0}\left(\frac{1}{\gamma^2}-\frac{1}{\gamma}\right)\right] = \ln\frac{K_s+1}{K_d{}^0K_s} + \frac{P}{[H_2O]_0} + \ln\left(1+\frac{1}{K_0(K_s+1)[H_2O]_0}\right) \quad (23)$$

The K values ($1/K_d + 1/K_dK_0[H_2O]_0$ for $Pt(PEt_3)_3$, $1/K_d + 1/K_dK_s + 1/K_dK_sK_0[H_2O]_0$ for $Pt[P(i\text{-}Pr)_3]_3$) at $[H_2O]_0$ of 5.549 M estimated from the slope of Fuoss plots (eq 21 and Figure 7) were 2.2 (0.7) $\times 10^2$ M^{-1} for $Pt(PEt_3)_3$ and 9.2 (2.0) $\times 10^2$ M^{-1} for $Pt[P(i\text{-}Pr)_3]_3$. These are in fair agreement with the respective values of 2.6 (0.2) $\times 10^2$ and 9.9 (2.0) $\times 10^2$ M^{-1} calculated on the basis of K_0, K_d, and K_s values assessed (see text).

References and Notes

(1) E. L. Muetterties, "Transition Metal Hydrides", Marcel Dekker, New York, 1971.
(2) M. A. Bennett and D. L. Milner, *J. Am. Chem. Soc.*, **91**, 6983–6994 (1969).
(3) M. A. Bennett and T. Yoshida, *J. Am. Chem. Soc.*, **100**, 1750–1759 (1978).
(4) T. Yoshida and S. Otsuka, *J. Am. Chem. Soc.*, **99**, 2134–2140 (1977).
(5) R. Zanella, F. Canizjani, R. Ros, and M. Graziani, *J. Organomet. Chem.*, **67**, 449–454 (1974).
(6) K. A. Azam and A. J. Deeming, *J. Chem. Soc., Chem. Commun.*, 852–853 (1976).
(7) C. R. Eady, B. F. G. Johnson, and J. Lewis, *J. Chem. Soc., Dalton Trans.*, 838–844 (1977).
(8) R. D. Gillard, B. T. Heaton, and D. H. Vanghan, *J. Chem. Soc. A*, 3126–3130 (1970).
(9) D. H. Gerlach, A. R. Kane, G. W. Parshall, and E. L. Muetterties, *J. Am. Chem. Soc.*, **93**, 3543–3544 (1971).
(10) B. N. Chaudret, D. J. Cole-Hamilton, R. S. Nohr, and G. Wilkinson, *J. Chem. Soc., Dalton Trans.*, 1546–1557 (1977).
(11) M. A. Bennett and T. G. Appleton, *J. Organomet. Chem.*, **55**, C88–C90 (1973).
(12) T. Yoshida, T. Okano, and S. Otsuka, *J. Chem. Soc., Dalton, Trans.*, 993–999 (1976).
(13) T. G. Appleton and M. A. Bennett, *Inorg. Chem.*, **17**, 738–747 (1978).
(14) T. G. Appleton, H. C. Clark, and L. E. Menzer, *Coord. Chem. Rev.*, **10**, 335–422 (1973).
(15) S. Otsuka, T. Yoshida, M. Matsumoto, and K. Nakatsu, *J. Am. Chem. Soc.*, **98**, 5850–5858 (1976), and references cited therein.
(16) R. Schunn, *Inorg. Chem.*, **15**, 208–212 (1976).
(17) T. Yoshida, Y. Ueda, and S. Otsuka, *J. Am. Chem. Soc.*, **100**, 3941–3942 (1978).
(18) L. J. Guggenberger, A. R. Kane, and E. L. Muetterties, *J. Am. Chem. Soc.*, **94**, 5665–5673 (1972).
(19) L. Malatesta and C. Cariello, *J. Chem. Soc.*, 2323–2328 (1958).
(20) F. A. A. Elhatez and D. J. Cram, *J. Am. Chem. Soc.*, **74**, 5851–5858 (1952).
(21) G. Johnes and B. C. Bradshaw, *J. Am. Chem. Soc.*, **55**, 1780–1800 (1933).
(22) C. A. Tolman, W. C. Seidel, and L. W. Gosser, *J. Am. Chem. Soc.*, **96**, 53–60 (1974).
(23) J. J. Zuckerman, *J. Chem. Educ.*, **42**, 315–317 (1965).
(24) C. A. Tolman, *J. Am. Chem. Soc.*, **92**, 2956–2965 (1970).
(25) C. A. Reed and W. R. Roper, *J. Chem. Soc., Dalton Trans.*, 1014–1020 (1973).
(26) T. E. Hogen-Esch and J. Smid, *J. Am. Chem. Soc.*, **88**, 318–324 (1966).
(27) "Handbook of Chemistry and Physics", 57th ed., CRC Press, Cleveland, Ohio, 1976–1977.
(28) R. M. Fuoss and F. Accasina, "Electrolytic Conductance", Interscience, New York, 1959.
(29) R. M. Fuoss, *J. Am. Chem. Soc.*, **80**, 5059–5061 (1958).
(30) C. A. Tolman, *Chem. Rev.*, **77**, 313–348 (1977).
(31) B. Rickborn, *J. Am. Chem. Soc.*, **84**, 2414–2417 (1962).
(32) N. Yoshimura, S. I. Murahashi, and I. Moritani, *J. Organomet. Chem.*, **52**, C58–C60 (1973).
(33) M. A. Bennett and R. Watt, *Chem. Commun.*, 95–96 (1971).
(34) R. J. Hodges and J. L. Garnett, *J. Catal.*, **13**, 83–98 (1969).
(35) M. A. Bennett, G. B. Robertson, P. O. Whimp, and T. Yoshida, *J. Am. Chem. Soc.*, **95**, 3028–3030 (1973).
(36) J. Smidt, T. Sieber, W. Hafner, and R. Jira, *Chem. Abstr.*, **62**, 447 (1965).
(37) M. A. Bennett and T. Yoshida, *J. Am. Chem. Soc.*, **95**, 3030–3031 (1973).
(38) For example, the ν(CO), ν(C≡N), and ν(N≡C) of *trans*-$[Pt(CH_3)(L)(PMe_2Ph)_2]^+$ (L = CO, C_2H_5CN, $CH_3OC_6H_4NC$) occur at higher frequencies compared to those of the corresponding CF_3 complexes.[39]
(39) T. G. Appletone, M. H. Chisholm, H. C. Clark, and L. E. Manzer, *Inorg. Chem.*, 11, 1786–1794 (1972).
(40) P. Beronius, *Acta Chem. Scand.*, **23**, 1175–1180 (1969).
(41) H. Hartley, N. G. Thomas, and M. P. Applebey, *J. Chem. Soc.*, **93**, 538–560 (1908).
(42) P. Walden, H. Ulich, and G. Bush, *Z. Phys. Chem. (Leipzig)*, **123**, 429–476 (1926).
(43) P. Walden and E. J. Birr, *Z. Phys. Chem. (Leipzig)*, **153**, 1–51 (1931).

Electron-Transfer Reactions of Metallocenes. Influence of Metal Oxidation State on Structure and Reactivity

John D. L. Holloway and William E. Geiger, Jr.*

Contribution from the Department of Chemistry, University of Vermont, Burlington, Vermont 05401.

Received June 5, 1978

Abstract: Vacuum- and low-temperature electrochemical techniques have been used to characterize the redox pathways of Cp_2V (Cp = η^5-cyclopentadienyl), Cp_2Cr, Cp_2Ni, Cp_2VCl_2, and $CpNi(\eta^3\text{-}C_5H_7)$. The pure metallocenes show an electron-transfer series of three or four members. The nickelocene anion, a d^9, 21-electron species, was shown to be a reduction intermediate, stable in DMF at −60 °C, and $CpNi(\eta_3\text{-}C_5H_7)$ was but a minor product of the bulk reduction of nickelocene. The heterogeneous electron-transfer rate was abnormally slow for the nickelocene reduction, suggesting that a structural distortion and/or a change in solvation occurs to relieve the high metal electron density. Vanadocene was oxidized in two one-electron steps, only the first of which was reversible. It is unlikely that there are gross changes in structure in going from vanadocene to the vanadocene cation, but the irreversibility of the second oxidation suggests the formation of $Cp_2V(THF)_2{}^{2+}$ for the d^1 species.

Introduction

The bis(η^5-cyclopentadienyl)metals, the "metallocenes" (**1**), are the prototype of organometallic π complexes, and have been widely studied since the discovery of ferrocene in 1951.[1] One of the most interesting aspects of these molecules is their ability to form compounds in violation of the 18-electron rule so commonly employed in organometallic chemistry.[2] Neutral compounds of the familiar sandwich structure are known for all first-row transition metals between V (15 valence electrons) and Ni (20 valence electrons). Because of this ability to accommodate a variable d-orbital occupancy, these compounds appeared to be likely candidates for investigation of electron-transfer reactions of organometallic π compounds. Electron-transfer series encompassing four or more members have been

0002-7863/79/1501-2038$01.00/0